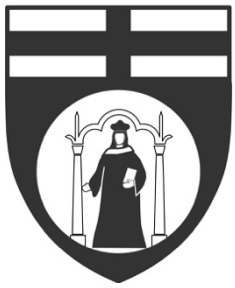

UNIVERSITÀ DEGLI STUDI DI GENOVA

Scuola di Dottorato in Biotecnologie in Medicina Traslazionale

XXXII Ciclo

(curriculum medicina rigenerativa)

Doctoral School of Biotechnologies in Translational Medicine

XXXII Cycle

(curriculum regenerative medicine)

"Functional characterisation of the SH3BGRL3 protein"

Tutor:
Fabio Giuseppe Ghiotto

PhD Candidate:
Filippo Di Pisa

Academic year: 2018/2019

To my brother.

Contents

ABSTRACT

SH3-domain **B**inding **G**lutamic acid **R**ich **L**ike **3** (SH3BGRL3) belongs to the SH3BGR family, it is ubiquitously expressed and encodes for a 93 AA thioredoxin-like evolutionary conserved protein. Its altered expression and tumor promoting role were described in certain malignancies e.g. lung, papillary and urothelial cancer. SH3BGRL3 shows a significant homology with *Escherichia coli* Glutaredoxin 3 however it is devoid of potential redox enzymatic activity, lacking the enzymatic site. This suggests some possible role as a modulator of GRXs activities or other proteins (e.g. its potential binding to Grb2 adaptor or EGFR proteins was emphasized in certain cell lines).

Our previous co-immunoprecipitation experiments demonstrated that SH3BGRL3 (and SH3BGRL as well) is able to interact Myo1c (via IQ domains) motor protein in SKBR3 cell line. Here we investigated the involvement of Ca^{2+} on the condition of this binding through pull-down experiments in SKBR3 cell lysates, the localization of the SH3BGRL3/Myo1c complex in MDA-MB-231 model and further functional role of SH3BGRL3 protein in correlation with tumor cell growth, survival and metastatic behavior were studied. Co-IP, pull-down, genetic modification (over-expressing and silencing) experiments, cellular localization studies, Western blots analysis, migration and invasion assays, metabolic analysis and tamoxifen sensitivity assays were performed in selected breast cancer cell lines (SKBR3, MDA-MB-231 and MCF-7) in order to investigate the functional role of the SH3BGRL3 protein.

In this work, the Ca^{2+} dependence of SH3BGRL3/Myo1c interaction were highlighted in SKBR3. The SH3BGRL3/Myo1c complex formation was also investigated in the highly invasive MDA-MB-231 cell line. However, such ability to complex formation of SH3BGRL/Myo1c could not be detected in this cell line, differently from what we sound in SKBR3 model. Moreover, our

results could not confirm that SH3BGRL3 (or SH3BGRL) interact with ErbB2, EFGR or Grb2 protein adaptor. In addition, the SH3BGRL3/Myo1c/actin complex formation and the role of SH3BGRL3 in cell motility, migration and invasion were shown in the MDA-MB-231 cell line. This motility regulatory function was SH3BGRL3 protein specific in our model, e. g. the other member of the protein family SH3BGR (e.g. SH3BGRL) had no such effect and was not able to co-immunoprecipitate with Myo1c. It was an interesting observation that Myo1c is detectable in exosomes isolated from MDA-MB-231 suggesting this protein as a potentially useful exosomes marker.

The specific tumorigenic roles of the SH3BGRL3 protein were further confirmed using SH3BGRL3 negative MCF-7 cell line in our experiments. Decreased ERα, increased motility and metabolic alterations (elevated mitochondria oxidation and glycolytic function) were detected in case of SH3BGRL3 over-expression in genetically modified MCF-7 cells. In parallel with these, 4'OH-TAM sensitivity was reduced in vitro compared to control MCF-7.

Based on these findings, SH3BGRL3 protein expression could influence cell motility, cell invasiveness and it could be involved in resistance against the hormone therapy of breast cancer cell lines.

INTRODUCTION

The completion of the "human genome" project in the early 2000s led to the identification of all human genes and the grouping of many of them into gene families based on significant homologies in the amino acid sequence. Over a decade later, however, the functional role of a substantial number of genes and genetic families remains in part or completely to be defined.

The *SH3BGR* gene

The *SH3BGR* gene (SH3 domain Binding Glutamic acid Rich) was identified and characterized during a project that had as its objective the construction of a transcriptional map of the region of chromosome 21 involved in the pathogenesis of congenital cardiopathies characteristic of Down Syndrome [1,2] . During the early stages of the embryonic development of the mouse, *SH3BGR* is selectively expressed in the heart while in later stages the expression appears extended to the striated musculature and to the smooth muscles of some organs such as the urinary bladder [3].

SH3BGR encodes for a mostly cytosolic protein of 174 amino acids characterized by a high conserved N-terminal domain and a C-terminal domain enriched in glutamic acid residues. Within the N-terminal domain there is a sequence enriched in proline (PLPPGIF) which contains a potential binding motif for the SH3 domain (consensus sequence: PXXP) [4] and one for the specific EVH1 domain of the Homer proteins [5].

SH3BGR effect on the cardiac morphogenesis process has been studied in a mouse model in which the *SH3BGR* gene expression in the heart has been increased to levels similar to those found in human trisomy 21. That study did not find the presence of cardiac malformations correlating the entire expression portrait of SH3BGR [2]. A study conducted recently on *Xenopus leavis* has shown that the extinction of *SH3BGR* expression influenced the

alterations in the development of sarcomeres and in the formation of the heart [6].

Since the C-terminal domain has an α-helix conformation, it seems to be able to bind calcium in a similar way to calsequestrin (in the endoplasmic reticulum) [7], through the high content of glutamic acid residues [1]. The domain for the binding of SH3, in the proline-rich region, is a very conserved sequence important for protein-protein interaction and for signal transduction processes. The understanding of the correct intracellular localization of the protein encoded by the *SH3BGR* gene and the identification of the proteins that interact with it remains a field of investigation still open, but that could provide important data on its function and on the correlation between a hyper-expression of this protein and the development of congenital cardiac diseases that characterize many subjects with Down Syndrome [8].

Following the characterization of the SH3BGR gene [9], three new genes have been identified that encode for small proteins called SH3BGRL [10], SH3BGRL2 [11] and SH3BGRL3 [12], which show a high homology with the N-terminal region of SH3BGR but lack the C-terminal region (**Figure 1**). The subsequent identification and characterization of *SH3BGR*-like genes [12] defined a new genes family coding for small proteins belonging to the Thioredoxin (Trx) superfamily, but lacking the CXXC sequence that characterizes their active site.

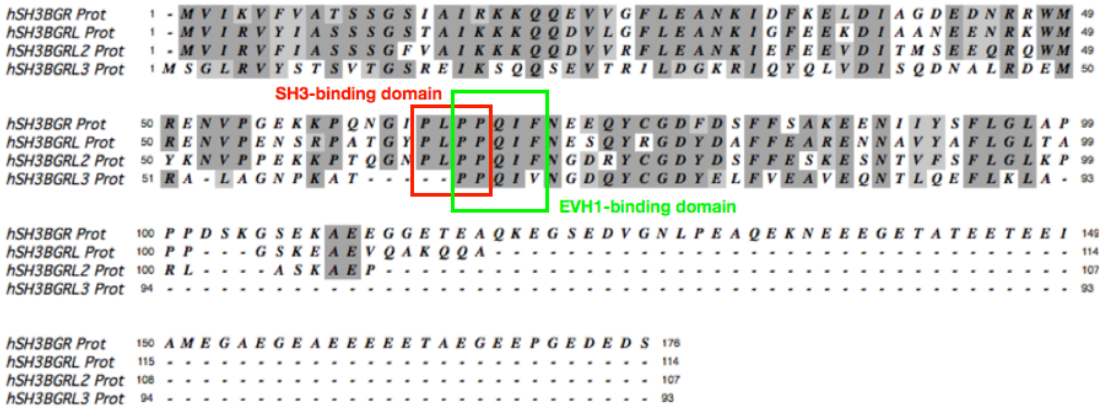

Figure 1. Human SH3BGR family proteins amino acids sequence alignment. The homology among the four protein is high, especially at the N-terminal domain. SH3BGR, SH3BGRL and SH3BGRL2 are considerably conserved, while SH3BGRL3 shows some differences in the amino acid sequence. SH3BGR has a long C-terminal domain that lacks in the other SH3BGR family members. The SH3- binding domain is boxed in red and the Homer EVH1- binding domain boxed is in green. Identical amino acids are shaded in dark grey while conservative substitutions are in light grey.

The *SH3BGRL* gene

The *SH3BGRL* (SH3BGR Like) gene is located on the X chromosome, in the q13.3 region. *SH3BGRL* is expressed ubiquitously, not only in muscle tissue such as *SH3BGR*, and encodes for a cytoplasmatic protein of 114 amino acids (smaller than that encoded by *SH3BGR*) that preserves the region rich in proline containing the binding regions for the SH3 and the EVH1 domains [10]. Indeed, SH3BGRL shares a 60% identity of amino acids and 84% of amino acid convervation level with the N-terminal region of SH3BGR protein. The N-terminal of SH3BGRL also appears to be highly conserved, sharing 95% identity with the mouse homologue protein(**Figure 2**). Majid and co-workers [13] have demonstrated that the suppression of *SH3BGRL* gene plays an important role in the neoplastic transformation induced by the oncogene *v-rel* in lymphatic cells and in chicken fibroblasts. Restoring the normal expression of SH3BGRL reduces the transforming capacity of *v-rel* by 76%. In mice, SH3BGRL (mSH3BGRL) seems to play a role in cell invasion in vitro and tumor metastasis through its binding with c-Src oncogene promoting its activation

though human SH3BGRL (hSH3BGRL) shows a tumour suppressor activity [14].

Moreover, Muniz Lino and collaborators [15] identified SH3BGRL among the sixteen proteins whose expression is most increased in samples of triple negative breast cancer, characterized by poor response to therapies and high invasive capacity.

Quantitative changes in the SH3BGRL expression have also been described in neurodegenerative disorders: in a study of the cells belonging to the substantia nigra in subjects with Parkinson's disease, Werner and colleagues identified SH3BGRL among the proteins which expression is significantly increased in diseased cells [16]. An increased expression of SH3BGRL has also been described in brain tissue of patients with Alzheimer's disease and fibroblasts from subjects with presenilin mutations 1 [17].

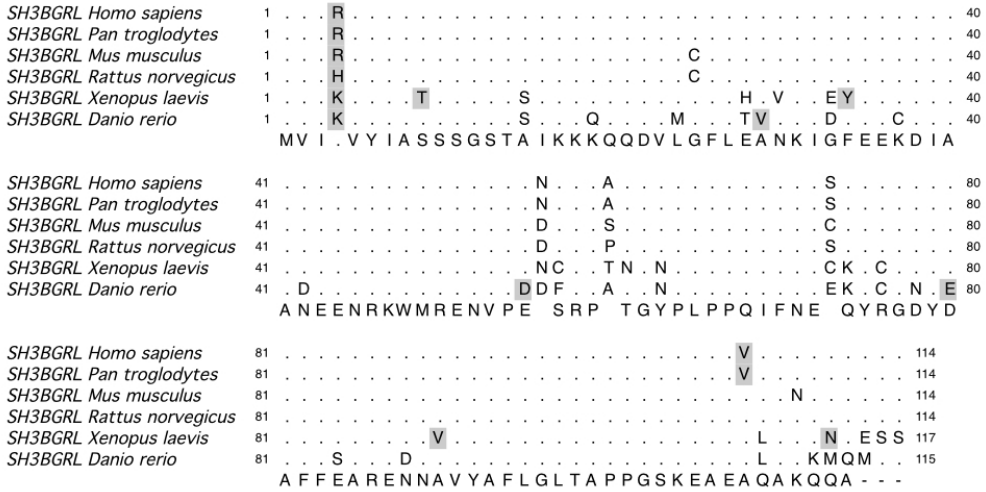

Figure 2. SH3BGRL protein sequence alignment. SH3BGRL shows high homology among different species. Dots represents identical amino acids. SH3BGRL from *Mus musculus* (mSH3BGRL) and *Homo sapiens* SH3BGRL (hSH3BGRL) show a high identity though Wang et al. [15] found an opposite between mSH3BGRL and hSH3BGRL.

The *SH3BGRL2* gene

The *SH3BGRL2* (SH3BGR Like 2) gene is located on chromosome 6 in the q13-15 region, it encodes a protein of 107 amino acids which, like the SH3BGRL protein, it shows a high homology with the N-terminal region of SH3BGR and it is very similar to the glutaredoxin present in *E. coli*.

SH3BGRL2 shows 63% identity and 83% similarity with the N-terminal region of SH3BGR; 63% identity and 79% similarity with SH3BGRL, and 39% identity and 60% similarity with SH3BGRL3. Like SH3BGRL and SH3BGRL3, the SH3BGRL2 protein also lacks the C-terminal sequence rich in glutamic acid [10].

SH3BGRL2 gene generates transcripts of approximately 3 and 5 kb, characterized by a particularly extensive and untranslated 3 'regions rich in AUUUA repetitions (AU Rich Elements, AUREs) that are related to the rapid degradation of messenger RNA [17]. The tissue distribution of SH3BGRL2 expression was seen to be abundant in the brain, placenta, liver and kidney. An interesting aspect of SH3BGRL2 is its expression in the retina, an expression that is elevated in the fovea. A molecular analysis on differential expression in cones and rods has shown that SH3BGRL2 transcripts are present exclusively in cones. The peculiar expression and chromosomal localization makes SH3BGRL2 a potential candidate for the pathogenesis of familial forms of retinal degeneration [18].

Regarding the cellular localization of the SH3BGRL2 protein, positive signals have emerged from the nucleus and from the perinuclear region.

Recently, SH3BGRL2 protein has been found as a tumor suppressor and modulator of cell growth and metastasis in clear cell renal carcinoma via activating hippo/TEAD1-Twist1 pathway [19].

The *SH3BGRL3* gene

The *SH3BGRL3* (SH3BGR Like 3) gene is mapped to chromosome 1p34.3-35. *SH3BGRL3* encodes for a small protein of 93 amino acids, ubiquitously expressed, characterized by a high degree of evolutionary conservation [12]. Compared to the other SH3BGR members family, SH3BGRL3 protein shows slight differences: 39% identity and 76% similarity to the N-terminal SH3BGR protein region; 42% identity and 73% similarity to the SH3BGRL protein.
The most important aspect that differentiates SH3BGRL3 from other proteins in the family is the modification of the proline-rich sequence with the consequent loss of potential binding sites for the SH3 and EVH1 domains.
The analysis of the amino acid sequence shows a significant homology with the *Escherichia coli* glutaredoxin 3; however SH3BGRL3 is completely devoid of the CXXC sequence which is present in all glutaredoxin proteins and constitutes the active enzymatic site. SH3BGRL3 is therefore devoided of potential redox enzymatic activity. The structure of SH3BGRL3 was solved by crystallization [20] and NMR [21] techniques.

Glutaredoxins (GRXs) are ubiquitous GSH-dependent oxidoreductases that provide the regulation of cellular process associated with changes in the redox state [21]. Structurally, GRXs belong to the TRx superfamily and the common domain consists of a four stranded ß-sheet surrounded by three α-helices and all oxidoreductase proteins share a similar active site motif (Cys-X-X-Cys or Cys-X-X-Ser) located between ß-sheet 1 and α-helix 1. As GRXs, also SH3BGRL3 presents the same domain formed by four stranded ß-sheet surrounded by three α-helices.
The SH3BGRL3 protein is characterized by a carboxyl-terminal half of about 60 amino acids, that shows significant sequence identity (21–33%) with the corresponding regions of *Escherichia coli* GRX1 and GRX3, and with human and pig liver GRXs (**Figure 3**). On the contrary, the N-terminal sequence of SH3BGRL3 differs from those of *E. coli* and mammalian GRXs, lacking both

Cys residues essential for the enzymatic activity in GRXs. Indeed, SH3BGRL3 is devoid of redox enzymatic activity and this suggests a possible role of the SH3BGRL3 protein as a modulator of GRXs activities by competitive binding to target proteins [21].

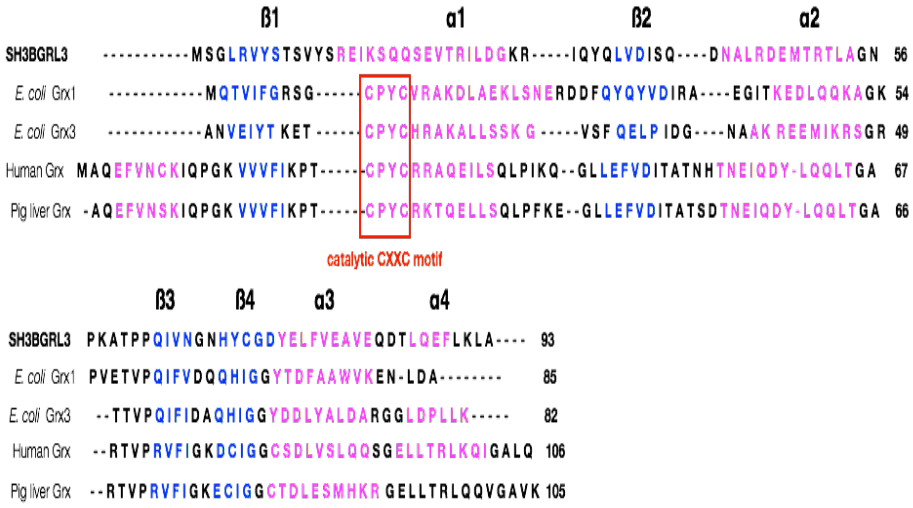

Figure 3. Amino acids sequence alignment of the SH3BGRL3 protein with *E. coli* GRX1, *E. coli* GRX2, Human GRX and Pig liver GRX proteins. Residues assuming ß-sheet and α-helix conformations are in blue and pink, respectively. The GRX residues of the catalytic CXXC motive are boxed in red.

Modifications of SH3BGRL3 expression have been related to the invasive capacity of different tumour forms. Recently, SH3BGRL3 has been identified among the markers of negative prognosis in lung adenocarcinoma [23], papillary thyroid cancer [24] and in the secretome from osteoblasts derived from sclerotic subchondral bone in osteoarthritis [25] suggesting SH3BGRL3 to be a secreted protein as a potential prognostic biomarker of these types of tumor.

Chiang et al [26] have shown that an increase of SH3BGRL3 expression correlates with an increased invasive capacity in uro-epithelial carcinoma, associating its expression with epithelial-mesenchymal transition (EMT), cell migration, cell proliferation and an increased risk of tumor progression in patients with non-invasive cancer. They found that the SH3BGRL3 protein

interacts with Epidermal Growth Factor Receptor (EGFR) at Y_{1068}, Y_{1086} and Y_{1172} trough Grb2 adaptor protein. The interaction between Grb2 and SH3BGRL3 is hypothesized to occur through SH3BGRL3 proline-rich motif even although SH3BGRL3 does not have a canonical SH3-binding domain [12].

Interesting is the identification of SH3BGRL3 mRNA at the level of membrane protrusions related to the invasion process in the breast cancer line MDA-MB-231 [28].

As with SH3BGRL, expression levels of the SH3BGRL3 protein were also found to be increased in fibroblasts from patients with familial Alzheimer's disease due to Presenilin-1 mutations [18].

SH3BGRL3 results to be very conserved along many species including those far from humans, like *Xenopus Laevis* and *Danio rerio* (**Figure 4**) suggesting a possible common and important role of the SH3BGRL3 protein in the biology of these organisms.

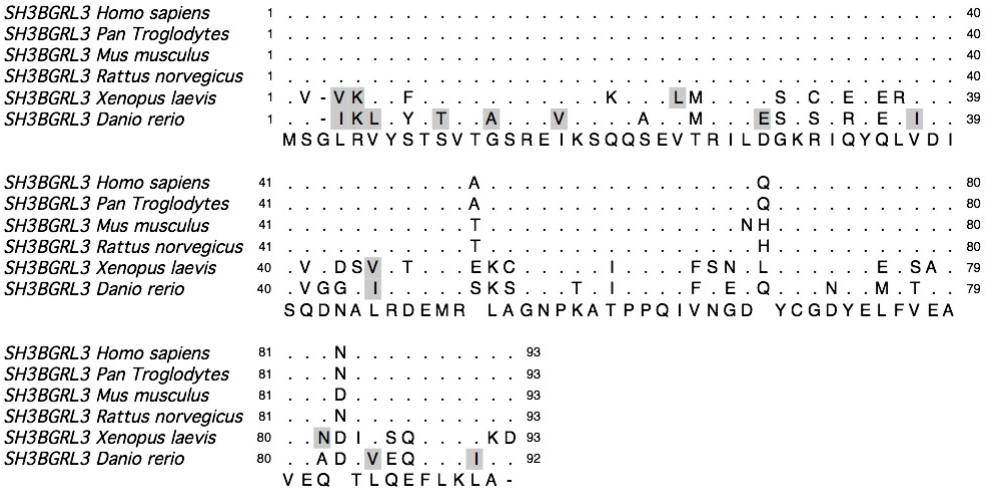

Figure 4. The SH3BGRL3 protein sequence alignment. SH3BGRL3 shows high homology in different species. Dots represents identical amino acids.

Myosin family

Myosins belong to a big family of ATP-dependent motor proteins associated to the cytoskeleton and able to “move” along actin filaments, typically from the minus end of them (depolymerisation) to the plus end (polymerization), except for myosin IV which progresses from the plus end to the minus end [29].
They are usually huge proteins that can act as homodimers (e.g. myosin II) or they can form a complex with other proteins. They mediate many cell functions, from cell movement and muscle contraction to the translocation of vesicles along the cytoskeleton and cell membrane remodelling (e.g. endocytosis and exocytosis, lamellipodia and pseudopodia formation), all of them driven by hydrolyzing ATP to ADP and moving along actin filaments [30].
The myosin family counts at least 35 distinct groups but they share a common structure. This structure is made by:
i) a catalytic motor domain (“head”) at the N-terminal. This globular domain has two important binding sites: one is the region that contacts the actin and the other one is the ATP motif that can hydrolyze ATP in ADP+Pi, generating the mechanical force necessary to change its conformation and slide along the actin filaments; ii) a central region (“neck”) that acts as a linker and as a lever arm allowing the motor domain to spread the force generated by the ATP hydrolysis to the tail. The neck is made by a repetition of IQ domains [31] and it is often associated to calmodulin (CALcium-Modulated protein, CaM) [32] or other light chains proteins (called Light Chain-Binding Domain) that can bind myosins or build a macromolecular complex with a regulatory function; iii) a C-terminal domain (“tail”) that contains specific domains able to bind vesicles, cell membranes (via lipids) even other myosins proteins. The ability of this region to bind different molecules depend on the specific kind of myosin.

The best known member of the family, and the first to be described, is the myosin II (defined a “conventional myosin), whose function is carried in muscular cells. Subsequently, other myosins have been characterized as

"unconventional myosins" and they are classified between class I and class XVII [33].

Myosin 1c

Myosin 1C (Myo1c) belongs to the class 1 myosins. They are all single chain molecules, most of them are ubiquitously expressed (1B, 1C, 1D and 1E) and others are tissue specific (e.g. 1A is expressed in the gut, while 1E and 1F are expressed in the hematopoietic cells). Eight different subtypes have been described (**Figure 5**) and each of them contains the motor domain at the N-terminal, the "neck region" consisting of several IQ calmodulin-binding motifs and the "tail region" at the C-terminal. In all of them the "tail region" contains a Tail Homology 1 (TH1) domain, followed by a Pleckstrin Homology (PH) domain able to bind membrane lipids (as phosphatidylinositol 4 5-bisphosphate, PIP2). In addition, the long tail of myosin 1E and myosin 1F contains also a TH2 domain and a C-terminal SH3 domain as shown in the figure below. As "conventional myosins", all class 1 myosins are also able to bind the actin cytoskeleton [34].

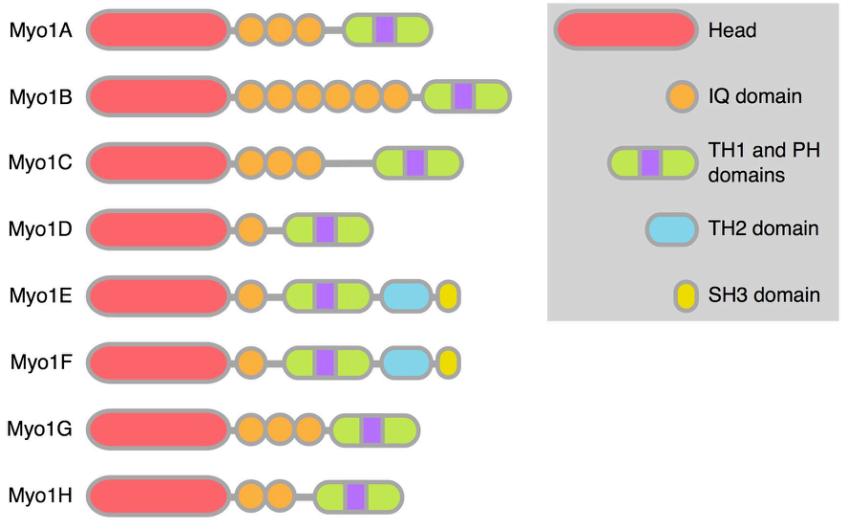

Figure 5. Schematic representation of class I Myosins. All the members are single chain molecules having a N-terminal domain ("head", light red) able to bind actin cytoskeleton,

different IQ domains (orange) able to bind CaM or other Light Chain-Binding Domain and a C-terminal domain ("tail"). The tail is made by a TH1 domain (light green) and a PH domain (purple). Some of these myosins present also two additional domains: a TH2 domain (light blue) and a SH3 domain (yellow).

Myosin 1C (encoded by *Myo-1c* gene localized on chromosome 17p13.3) is a 1063 amino acids protein initially described as a nuclear myosin. Myo1c shares a common structure with all others myosins (**Figure 6**): the N-terminal "head region" is 700 amino acids long, the "neck region" 90 amino acids and C-terminal "tail region" about 270 amino acids long. The "tail region" is made by three IQ domains (named IQ1, IQ2 and IQ3) followed by a post-IQ region made by three α-helices (named α2, α3 and α4) [35]. IQ domains are basic, often amphipatic α-helices consisting of approximately 20 amino acids. For myosins, the IQ motif consensus sequence is IQXXXRGXXXR [36]. Myo1c 1Q region binds CaM, calmodulin-like proteins with EF-domain (e.g. Calcium-Binding Protein 1, CaBP1 and Calcium- and integrin-binding-protein1, CIB1) and others light chain-binding proteins (LCBD) [37].

CaM binds Myo1c IQ domains in presence of a low concentration of Ca^{2+} determining an increase of the stability in myosin 1c "neck region", essential during the *coup de force* to transduce the tension generated by motor domain to the "tail region". When Ca^{2+} concentration in the cell rises, CaM dissociates from IQ domains (binding Ca^{2+} through its EF-hand domains) and determines more flexibility of the Myo1c "neck region" [38].

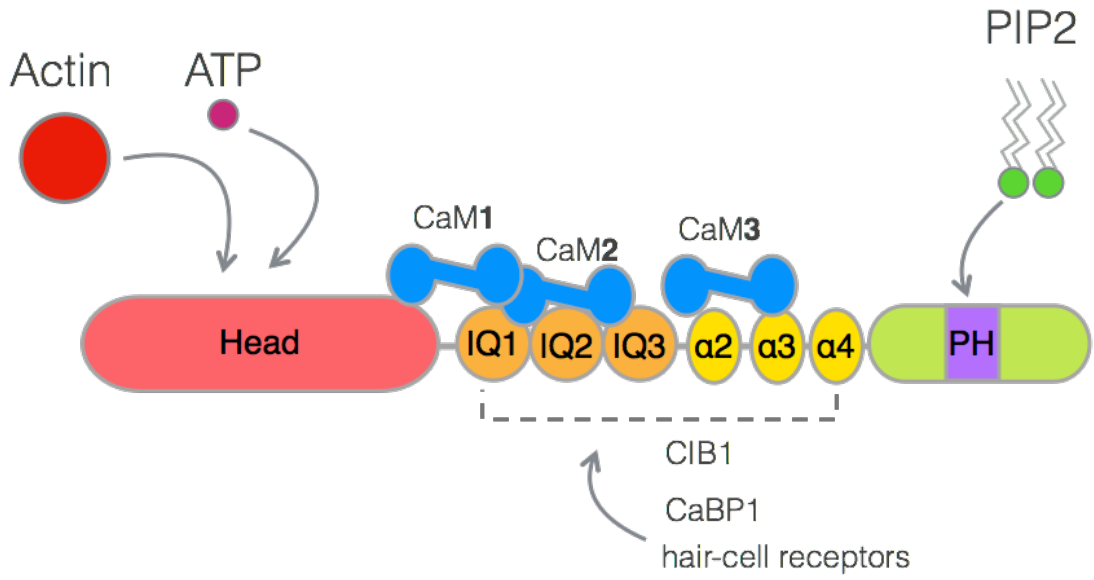

Figure 6. Myo1c Schematic representation. The "head region" (light red) binds ATP and actin while "tail region" (green) binds cell membrane through its PH domain (purple). The "neck region" is made by three IQ domains (orange) followed by a post IQ region (alpha-helices, yellow). According to recent papers, two CaM molecules interact with IQ domain 1 (partially also with the "head region" and 2; the third one with IQ3 domain, α2, α3 and partially α4 region.

Myo1c is expressed in most eukaryotic cells and it has been co-localized with actin-rich cell periphery along the plasma membrane. According to this, Myo1c results important in the communication between the inside of the cell and its environment transducing signals from cell membrane receptors to the cytoskeleton, exposing ionic channels on the plasma membrane in response to different stimuli, transporting vesicles from and to the plasma membrane and helping their release into the outside environment [39, 40, 41].

Myo1c shows also lots of specific functions in different specialized cell type. In the sensory hair cells of the inner ear, Myo1c is expressed in the stereocilia tips where it controls the tension of the tip links that connect neighboring stereocilia during the hair cell adaptation [42, 43, 44].

Myo1c facilitates the correct targeting of lots different cargoes from the cytoplasm to the plasma membrane, for examples Myo1c has been implicated in insulin-stimulated glucose transport 4 (GLUT4) trafficking and plasma membrane fusion via interaction with ReIA in adipocytes cell types [45, 46, 47].

Otherwise, Myo1c stabilizes actin at the Golgi complex, facilitating the arrival of incoming transport carriers at the Golgi in human cells [48]. Myo1c plays an important role in membrane remodelling, through membrane uptake (endocytosis) and balanced exocytosis of intracellular membranes [49], in lipid raft recycling [50], in autophagosome/lysosome formation and in pathogen internalization (e.g. *Salmonella*) [51]. Myo1c localizes at the growing membrane protrusions generated during B cells spreading and it is actively recruited to the immune synapse, showing co-localization with MCH-II [52]. Myo1c shows also an important role in the development of the grown cone of neurons axons and dendrites where Myo1c localizes in lamellipodia and filopodia [53]. Myo1c is also critical in the formation of lamellipodia and cell migration in the model of N1 glioblastoma [54]. All this data suggest Myo1c as a molecular motor universally involved in membrane trafficking, cargo delivery and cell motility [55].

RATIONALE

In 2005, Schulze at al. [56] published a proteomic work in which it was described the interaction patterns to all cytosolic phosphorylated tyrosine residues of all EGF-Receptor (Epidermal Growth Factor Receptor, or ErbB-receptors) family members. In this study, SH3BGRL (or SH3BGRL3, since the paper refers to SH3BGRL, while the Protein Data Bank number indicated in paper points to the SH3BGRL3 protein) has been founded to bind phosphorylated Y_{891} in ErbB1 (EGFR) and phosphorylated Y_{923} and phosphorylated Y_{1196} in ErbB2. According to this, we investigated the SH3BGRL and SH3BGRL3 role in EGFR signal transduction using the SKBR3 cell line, a breast cancer cell line over-expressing ErbB2 protein. After, Chiang et colleagues [13] revealed SH3BGRL3 able to interact directly with EGFR protein.

It is well known that members of the ErbB-receptors, that are ubiquitously expressed, play a crucial role in cell proliferation and differentiation. In particular, changes in expression and aberrant activation, especially for EGFR and ErbB2, are related to a variety types of breast cancer development and progression including metastasis [57, 58].

According to this data, we were interested to investigate better the role of SH3BGRL and SH3BGRL3 proteins in the EGFR signal pathway.

Since notwithstanding several by co-immunoprecipitations experiments no interaction between SH3BGRL (or SH3BGRL3) and the ErbB2 receptor could be demonstrated, we decided to analyse the co-immunoprecipitate of SH3BGRL3 in SKBR3 cell lysate by mass spectrometry analysis to identify any possible interactors. Mass spectrometry analysis of bands obtained by co-immunoprecipitation of FLAG tagged SH3BGRL3 protein [59], as we already demonstrated, revealed the proteins Myosin 1c, Adseverin and Actin as possible SH3BGRL3 binders. Our result from the co-immunoprecipitation reflects the common role of Myosin 1c, Actin and Adseverin proteins have in the turn-over of the Actin Cytoskeleton [60]. We focused our attention on

Myosin 1c and the mass spectrometry result was confirmed by co-immunoprecipitation assays in SK-BR-3 (previously transfected by FLAG-SH3BGRL3 as a bait).

After the demonstration of the SH3BGRL3 interaction with Myosin 1c, we investigated which part of Myosin 1c interacts with SH3BGRL3 protein and we demonstrated that essentially the “neck” region of Myosin 1c, composed by the IQ domains, is involved in this binding, suggesting SH3BGRL3 as a protein modulator of this region (like Calmodulin protein) [59, 61, 62].

In this study, we explore the binding conditions of SH3BGRL3 with the Myosin 1c and we propose a possible function of the SH3BGRL3 protein in cancer progression, exploring and analysing its expression in different type of breast cancer cell lines.

MATERIAL AND METHODS

Cell lines culture

Human breast cancer cells line SKBR3, MDA-MB-231, MDA-MB-468, MCF-7, T47D and BT-474 (American Type Culture Collection, ATCC) have been maintained in DMEM (Euroclone) containing 10% FBS (Life Technology, ThermoFisher), 1% L-Glutamine (Life Technology, ThermoFisher) and 1 mg/mL penicillin/streptomycin (Sigma) in 5% CO_2 humidified atmosphere (receptor status is shown in **Figure 7**). For exosomes isolation, the MDA-MB-231 cell line has been maintained in DMEM (Euroclone) containing 1% L-Glutamine (Life Technology, ThermoFisher) and 1 mg/mL penicillin/streptomycin (Sigma) in 5% CO_2 humidified atmosphere.

Cell line	Phenotype	ER	PR	HER2
SKBR3	Luminal *HER2*	-	-	+
MDA-MB-231	Tripl negative	-	-	-
MDA-MB-468	Tripl negative	-	-	-
MCF-7	Luminal	+	+	-
T47D	Luminal	+	+	+
BT-474	Luminal	+	+	+

Figure 7. Receptor status (for Estrogen Receptor, ER; Progesteron Receptor, PR; and ErbB2, HER2) of the breast cancer cell lines that we used in our experiments.

Construct synthesis

Constructs were built using In-fusion Cloning Kit (Clontech). We first amplified the DNA using Phusion Hot Start Flex DNA Polymerase (New England Biolabs) and a three-step PCR. Infusion Cloning Primers were designed including 15bp homologous to the ends of the linearized target vector. After PCR products running on agarose gel, we purified the sample using Exosap (Affimetrix). The recombination between the PCR product and the vector was performed using Infusion enzyme mix following the manufacturer's protocol. We used pFLAG-CMV and pIRESpuro for eukaryotic expression, while pGEX-6P-1 and pQE-30 are used for bacterial expression. For construct amplification, we transformed Stellar Competent Cells (Clontech) with Infusion products. Bacteria were grown in LB or in LB+Agar plates, both added with Ampicillin, at 37^{o}C. The screening of positive colonies was performed using DNA amplification; positive colonies were amplified and plasmids were extracted using Plasmid Miniprep kit (Machery & Nagel). A couple of plasmid for each construct was sequenced using the BigDye Sequencing kit (Thermo Fisher Scientific) to detect if there were any mutations. Selected clones were expanded and the vectors extracted using Plasmid Midiprep kit (Machery & Nagel).

Cell transfection

SKBR3 and MDA-MB-231 cell lines were transiently transfected, at 70-90% of confluence, with the different constructs using Lipofectamine 2000 (Life Technology, Thermo Fisher) according to the manufacturer's protocol. SH3BGRL and SH3BGRL3 silencing in MDA-MB-231 was performed using specific siRNA against *SH3BGRL* and *SH3BGRL3* genes (Ambion) while a scrambled siRNA (Ambion) was used as negative control.

To obtain a stable transfected cell line, the MCF-7 cell line was transfected using the Lenti-Pac^{TM} HIV Expression Packaging kit (GeneCopoeia^{TM}). Following the manufacturer's protocol, we first produced the virus using 293Ta lentiviral packaging cells (GeneCopoeia^{TM}) and then we transfected target

cells with pReceveir-Lv105-SH3BGRL3 and pReceveir-LV105 alone as a negative control. Selection of transfected cells has been done using puromycin antibiotic (Gibco,Thermo Fisher).

Cell lysis and Western blot

Cells were washed with PBS (Gibco, Thermo Fisher) and lysed, using a scraper, in EB buffer (Hepes 20mM, NaCl 150mM, glycerol 10%, Triton X-100 1%) or RIPA buffer (Sigma) added with Protease Inhibitors Cocktail (Sigma). Lysates were normalized on the basis of the total protein amount measured by Bradford assay (Biorad). Samples were run in SDS-PAGE on Mini-Protean TGX Precast Protein Gels (Biorad) using Colorbust Electrophoresis Marker (Sigma-Aldrich) and Leammli reducing buffer (Biorad). After electrophoresis, proteins were transferred on Hybond ECL Nitrocellulose Membrane (GE Healthcare) by Western blot technique. As primary antibodies, we used: α-SH3BGRL 1:1000 (Santa Cruz), α-SH3BGRL3 1:500 (Sigma-Aldrich), α-Myo1c 1:500 (Sigma-Aldrich), α-FLAG 1:1000(Sigma-Aldrich), α-GAPDH 1:5000 (Abcam), α-halix 1:200 (Santa Cruz), α-Tom20 1: 250 (Santa Cruz), α-ERα 1:1000 (Cell Signalling) and α-betaActin 1:3000 (Cell Signaling). We used goat α-mouse HRP 1:3000(Santa Cruz) and goat α-rabbit HRP 1:3000 (Santa Cruz) as secondary antibodies. To develop membrane, we used Amersham ECL Western Blotting Detection Reagent (GE Healthcare) and Amersham Hyperfilm ECL (GE Healthcare).

Protein production in bacteria

Codon Plus Competent Cells (Agilent Technology) were transformed with the plasmid of interest for bacterial expression. After screening, positive colonies were grown in LB broth + Ampicillin. Protein expression was induced with 0.1mM Isopropyl ß-D-1-thiogalactopyranoside (ITPG, Sigma) for 3 hours at 37^{o}C. Bacteria were lysed with a Sonicator in GST-buffer (Tris-HCl 1M pH 7,5, NaCl 4M, EDTA 200 μM, dH_2O). Recombinant protein was purified from the lysate using Sepharose-Glutathione 4B resin (GE Healthcare) After incubation

with the resin at 4°C overnight, recombinant protein was washed in GST-buffer and its molecular weight was detected by electrophoresis using SDS-page gels (Biorad) and Coomassie Brilliant Blue (Sigma-Aldrich) staining.

Co-IP experiments

SKBR3 and MDA-MB-231 cell lines were previously transfected with the constructs of interest. After 48 hours, cells were lysed as described before, the total proteins amount was normalized by Bradford assay and the same amount of total protein was incubated with the anti-FLAG M2 affinity gel resin (Sigma-Aldrich) previously equilibrated with EB-buffer. The binding assay was performed overnight at 4°C in agitation. To remove the unbound proteins, resin after incubation was washed five times with EB-buffer and centrifuged. Tagged proteins were detached using 10% SDS and proteins were loaded on SDS-page and detected using western blot by specific antibodies.

Pull-down experiments

For the pull-down assay, GST-SH3BGRL3 fusion protein was synthetized and bound to a Sepharose-Glutathione resin as previously described [57]. SKBR3 cell line was lysed and normalized to the total protein amount. The same amount of total proteins was incubated with GST-fusion protein overnight at 4°C in agitation. The binding was performed using EB-buffer added with $CaCl_2$ 1mM or with EGTA 5mM. Unbounded proteins were washed 5 times in EB-buffer (with $CaCl_2$ 1mM or with EGTA 5mM, respectively) and centrifuged. Tagged proteins were detached using 10% SDS and proteins were loaded on SDS-page and detected, using western blot, by specific antibodies.

Migration and Invasiveness assays

We tested migration and invasion capability after *SH3BGRL3* and SH3BGRL gene silencing in MDA-MB-231 cell line. We down-regulated SH3BGRL3 expression by using two different Silenced Select Pre-designed siRNA (Ambion). We also used a scrambled siRNA (Ambion) as a negative control.

Cells were plated in 6-wells plates (Corning) in DMEM + 10% FBS + 1% Pen/Strep + 1% Glutamax and after 24 hours from the plating, siRNAs were introduced in the cells by transfection using Lipofectamine 2000 (Thermo Fisher Scientific) according to the manufacture's protocol. 48 hours after cell transfection, cells were starved using DMEM + 1% Pen/Strep + 1% Glutamax without FBS. After 8-10 hours of starvation, 25'000 cells were seeded in Boyden Chambers (Migration Support for 24 Well Plate with Transparent PET Membrane 8.0 μM pore size, Corning) or in Transwell covered by Matrigel (BioCoat^{TM} Matrigel® Invasion Chambers PET Membrane 8.0 μM pore size, Corning). After 16 hours of migration, cells were removed from the top using Cristal Violet 1% (Sigma-Aldrich) and Glutaraldehyde 5% (Sigma-Aldrich), respectively [62]. Cells were counted in double-blind.

Immunofluorescence

After cell transfection with pCMV-FLAG/SH3BGR3 and pCMV-FLAG contructs, MDA-MB-231 cells were seeded on glasses for microscopy and fixed with Paraformaldehyde 3% (Sigma-Aldrich) before staining. For intracellular fluorescence, cell permeabilization was performed using Triton X-100 0,1% (Sigma-Aldrich). PBS (Invitrogen, Thermo Fisher) + BSA 0,5% (Sigma-Aldrich) was used as a washing buffer while PBS+ BSA 2% was used for the saturation. We used α-FLAG (Sigma-Aldrich), α-Myo1c (Sigma-Aldrich) and Phalloidin Alexa Fluor-488 (Sigma-Aldrich) as primary antibodies while Alexa Fluor 488 goat α-rabbit (Life Technology) and Alexa Fluor 546 goat α-rabbit (Life Technology) were used as secondary antibodies. DAPI (Abcam) was used for the nuclear stain.

Scratch assay

MCF-7 cells were grown in complete medium and seeded into 24-well tissue culture plate (Corning). At ca. 70-80% confluence as a monolayer, cells were starved for 12 hours in medium serum free. Gently and slowly, we performed the scratch using a 200μL pipette tip across the middle of the well. Wells were

washed with PBS to remove the detached cells and replenished with fresh complete medium. Pictures have been taken at time 0, 24 and 48 hours after the scratch. The gap distance was evaluated using ImageJ software and the % of the closure was calculate by the formula: *% of wound closure = [(Area$_{t=0h}$- Area$_{t=\Delta h}$)/ Area$_{t=0h}$] x100* [63].

Proliferation assay

Cell growth has been evaluated by the xCELLigence system (Agilent) real-time cell analysis (RTCA) via the measurement of cell-induced electrical impedance [64], following the manufacturer's protocol. 5'000 cells were seeded in E-Plate VIEW 16 (Agilent) covered by collagen (Sigma-Aldrich) and cell growth (Slope) was followed until 96 hours. In order to investigate the effect of the Tamoxifen, MCF-7 over-expressing SH3BGRL3 and control MCF-7 have been treated with 1μM of 4'OH-Tamoxifen (Sigma-Aldrich) dissolved in DMSO [65], 24 hours after plating. Medium has been changed every 48 hours and cell growth was followed until 200 hours from the plating.

Exosomes isolation from MDA-MB-231 cell line

At ca. 70% of confluence, complete culture medium was removed and cells were washed 3 times with sterile PBS (Thermo Fischer Scientific). DMEM (Thermo Fischer Scientific) was added without FCS and cells have been incubated for 72 hours and successively the supernatant was collected and centrifuged at 300g for 10 minutes at 4^{o}C to remove cells and debris. Subsequently, the supernatant was at 2'000g for 20 minutes, at 1'000g for 30 minutes at 4°C and finally 100'000g for 90 minutes at 4^{o}C, in order to pellet the exosomes. The supernatant was gently removed and the pellet resuspended in PBS. A final centrifugation was performed at 100'000g for 70 minutes at 4^{o}C. Once the supernatant was removed, the pellet containing the microvesicles was lysed in RIPA buffer (Sigma-Aldrich).

Mitochondria isolation from MDA-MB-231 cell line

MDA-MB-231 were grown in complete medium and mitochondria were isolated from $2x10^7$ cells. We performed a high-purity isolation using Qproteome™ Mitochondria Isolation Kit (QIAGEN) following the manufacturer's protocol. After purification, the mitochondria pellet was lysed using RIPA buffer (Sigma-Aldrich).

Mammosphere formation assay

A single cell suspension of control MCF-7 cells or SH3BGRL3 over-expressing MCF-7 cells was prepared using enzymatic (1x Trypsin-EDTA, Sigma-Aldrich), and manual disaggregation (25gauge needle) [66]. Cells were then plated at a density of 500 cells/cm^2 in mammosphere medium (DMEM-F12/ B27 / 20-ng/ml EGF/PenStrep) in non-adherent conditions in culture dishes coated with 2-hydroxyethylmethacrylate (poly-HEMA, Sigma-Aldirch). Cells were grown for 5 days and maintained in a humidified incubator at 37°C at an atmospheric pressure in 5% carbon dioxide/air (v/v). After 5 days for culture, spheres > 50 µM were counted using an eye piece graticule, and the percentage of cells plated which formed spheres was calculated and is referred to as percentage at mammosphere formation. Mammosphere assays were performed in triplicate and repeated three times independently.

Metabolic flux analysis

Extracellular acidification rates (ECAR) and real-time oxygen consumption rates (OCR) for MCF7 cells were determined using the Seahorse Extracellular Flux (XFe96) analyzer (Seahorse Bioscience). Briefly, 15'000 control MCF-7 cells and SH3BGRL3 over-expressing MCF-7 cells per well were seeded into XFe-96 well cell culture plates for 24h. Then, cells were washed in pre-warmed XF assay media (or for OCR measurement, XF assay media supplemented with 10mM glucose, 1mM Pyruvate, 2mM L-glutamine and adjusted at 7.4 pH). Cells were then maintained in 175 μL/well of XF assay media at 37^{o}C, in a non-CO_2 incubator for 1 hour. During the incubation time, 5μL of 80mM

glucose, 9μM oligomycin, and 1M 2-deoxyglucose (for ECAR measurement) or 10μM oligomycin, 9 μM FCCP, 10 μM Rotenone, 10 μM antimycin A (for OCR measurement), were loaded in XF assay y media into the injection ports in the XFe96 sensor cartridge. Measurements were normalized by protein content (SRB assay). Data sets were analyzed using XFe96 software and GraphPad Prism software, using one-way ANOVA and Student's t-test calculations [67].

Sulphorhodamine B (SRB) assay

For the normalization of the Metabolic flux analysis, the cell viability was measured by Sulphorhodamine B assay (SRB, Sigma-Aldrich). The assay is based on the measurement of cellular protein contents. Cells were fixed with 10% Trichloroacetic acid (TCA) for 1 hour at 4^{o}C, and were dried overnight at room temperature. Then, plates were incubated with SRB for 30 minutes, washed twice with 1% acetic acid and air dried for at least 1hour. Finally, the protein-bound dye was dissolved in a 10mM Tris, pH 8.8, solution and read using a plate reader at 540-nm.

Statistics

For statistical comparison between samples, the Mann-Whitney U test was used for unpaired sample data and the Wilcoxon signed-rank test for paired sample data. Analyses were performed using the GraphPad Prism statistical software (GraphPad Software Inc., La Jolla, CA). Data are represented as the mean ± standard error of the mean (SEM), taken over ≥ 3 independent experiments, with ≥ 3 technical replicates per experiment, unless otherwise stated. Statistical significance was measured using the t-test. $P \leq 0.05$ was considered significant.

RESULTS

SH3BGRL3 binds Myo1c in a Ca^{2+}-dependent manner

Since calmodulin (CaM) binds Myo1c IQ domains in a calcium-dependent manner [33] and we previously demonstrated that also the SH3BRL3 protein is able to interact with Myo1c IQ domains [59], we investigated if also the binding of SH3BGRL3 to Myo1c was calcium dependent. For that purpose, we performed Co-IP and pull-down assays on SKBR3 cell lysates with or without calcium to demonstrated if the binding between SH3BGRL3 and Myo1c requires Ca^{2+} for its formation. For Co-IP experiments, SKBR3 cell line was transiently transfected with FLAG-SH3BGRL3 constructs with the FLAG vector alone as a control. Lysates were incubated at different Ca^{2+} concentration, pulled down using an anti-FLAG resin and analysed by SDS-PAGE and western blotting. **Figure 8** shows that Ca^{2+} is able to influence the interaction between SH3BGRL3 and Myo1c since the intensity of the band related to the Ca^{2+} condition is clearly more intense than the one in the presence of EGTA.

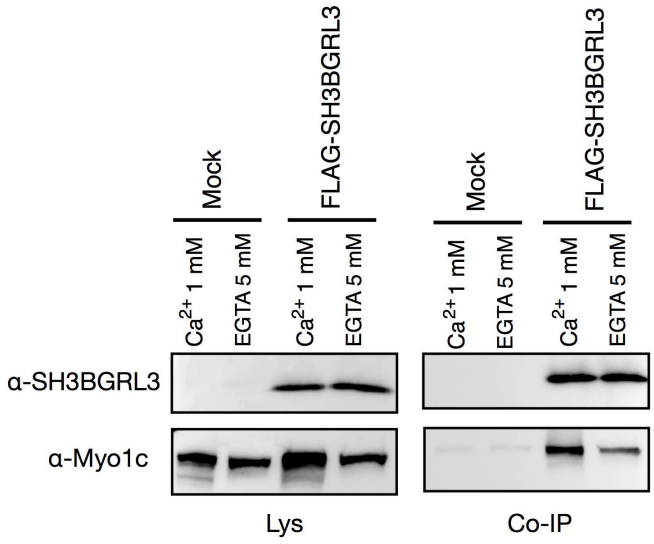

Figure 8 Co-IP using FLAG-SH3BGRL3 as a bait in SKBR3 cell line. Cells were transfected with pCMV/FLAG (Mock) and FLAG-SH3BGRL3. After Co-IP with anti-FLAG resin, in different Ca^{2+} concentration, samples were run on SDS-PAGE. We detected proteins using α-Myo1c and α-SH3BGRL3 antibodies. Lysates proteins are shown on the right and Co-IP proteins on the left. This experiment shows that there is a larger quantity of assembled SH3BGRL3/Myo1c

complexes in the presence of Ca^{2+}. It also shows that EGTA (a compound that sequesters Ca^{2+}) is not able to disassemble complexes that are already formed inside the cells before lysis.

However, since Co-IP assay is a technique that reveals mainly complexes already assembled inside the cell, it isn't the best choice to evaluate the formation of a new ones. For this reason, we performed a pull-down assay on SKBR3 lysates using recombinant GST-SH3BGRL3 and modulating the binding conditions (with EGTA or Ca^{2+}). According to this, we can simply justify the presence of a signal in the Co-IP with EGTA (**Figure 8** on the left) since this compound is not able to interfere with complexes already assembled inside the cell.

We first expressed a GST-SH3BGRL3 fusion protein using a construct (pGEX-6p-1/SH3BGRL3) suitable for bacterial expression carrying SH3BGRL3 preceded by a GST tag at the N-terminal of our protein and then we purified GST-SH3BGRL3 fusion protein using a Sepharose-Glutathione resin. We used the Glutathione-GST-SH3BGRL3 complex to pull-down Myo1c in wild type SKBR3 lysates at different Ca^{2+} concentrations. A Glutathione-GST alone has been used as a negative control. The result of the pull-down shows clearly that GST-SH3BGRL3 binds endogenous Myo1c in SKBR3 lysates in presence of Ca^{2+}, while the binding doesn't in the presence of EGTA. (**Figure 9**). The result of this experiment also indicates that the presence of EGTA in the Co-IP procedure (**Figure 9**, on the left) is not able to interfere with the complexes that are already assembled inside the cell.

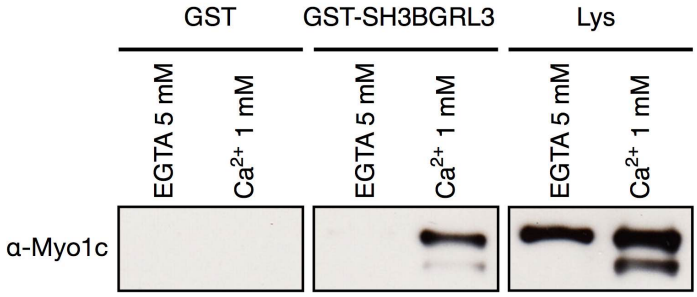

Figure 9. Pull-down of Myo1c in SKBR3 cell line by using GST-SH3BGRL3. Cells lysate were incubated with Glutathione-GST-SH3BGRL3 at different Ca^{2+} concentration (with Ca^{2+} or using EGTA to sequester Ca^{2+}). The samples were run on SDS-PAGE and proteins were detected in WB by using α-Myo1c antibody. Samples incubated with Glutathione-GST as negative control are shown on the left, followed by the pull-down results and lysates on the right.

These results clearly show that SH3BGRL3 binds Myo1c in a Ca^{2+}-dependent manner. Interestingly, also calmodulin binds Myo1c via neck region in a Ca^{2+}-dependent manner, but the CaM/Myo1c interaction occurs mostly in absence of Ca^{2+} [35, 37] whereas SH3BGRL3 binds Myo1c in presence of Ca^{2+}, suggesting a possible complementary role of calmodulin and SHBGRL3 in Myo1c "neck" region regulation.

Since Co-IP and pull-down experiments were made in the whole cell lysate containing lots of other proteins, we were interested to determine if the binding between SH3BGRL3 and Myo1c was direct or if there were other proteins mediating this interaction and to do this we planned to investigate the minimum binding conditions using only SH3BGRL3 and Myo1c as recombinant proteins in *in vitro* reactions. At first, we cloned *SH3BGRL3* gene into a pQE-30 vector tagged with a tail of six Histidine (His) at the N-terminal and we expressed his-SH3BGRL3 recombinant protein using the bacteria system followed by its purification using Nickel-NTA Agarose beads. Subsequently we cloned *Myo1c* gene into a pGEX-6-P-1 vector for the expression of a fusion protein tagged with a GST-tag at the N-terminal. The full GST-Myo1c recombinant protein production turned out to be very hard since just the only Myo1c is around 120 KDa and enriched of post-translation modification reveling it too complex for

the bacteria expression system. So we decide to synthesize a construct carrying only Myo1c “neck” region (IQ domains with a GST tag) that we previously demonstrated to be the Myo1c region involved in the interaction with SH3BGRL3 (data not shown). Also in this case, it was impossible to produce any “neck” region of Myo1c in the bacteria system and after lots of failed attempts to find out the best way to product the recombinant protein, the question if the interaction between SH3BGRL3 and Myo1c is direct or mediated by other protein is still opened.

SH3BGRL3 does not bind to pre-assembled SH3BGRL/Myo1c complexes

Since we previously found that SH3BGRL3 and SH3BGRL proteins were both able to interact with Myo1c in SKBR3 cell line (and in particularly that SH3BGRL3 binds Myo1c IQ domains) [59, 61, 62], we investigated if SH3BGRL3 and SH3BGRL proteins could be both present in the complex with the Myo1c. To do this we transfected SKBR3 cell line with the vectors pCMV/FLAG-SH3BGRL and pBiGFP/SH3BGRL3, with pCMV/FLAG-SH3BGRL alone as positive control and with pCMV/FLAG alone as negative control. Subsequently, transfected cells have been lysate and these lysates were incubated with an anti-FLAG resin to evaluate the binding with the Myo1c. We run samples on SDS-PAGE and detected proteins using specific antibodies α-Myo1c, α-SH3BGRL and α-SH3BGRL3. Western blot results (**Figure 10**) show that SH3BGRL is able to co-immunoprecipitate (Co-iP) Myo1c but not SH3BGRL3. This result reveals that the interaction between Myo1c and SH3BGRL is exclusive, not allowing its interaction with SH3BGRL3 which is also able to interact with Myo1c when it is not already involved in the interaction with SH3BGRL and this may suggest a different role of the SH3BGRL3 and SH3BGRL proteins on their regulation of the Myo 1c “neck region”.

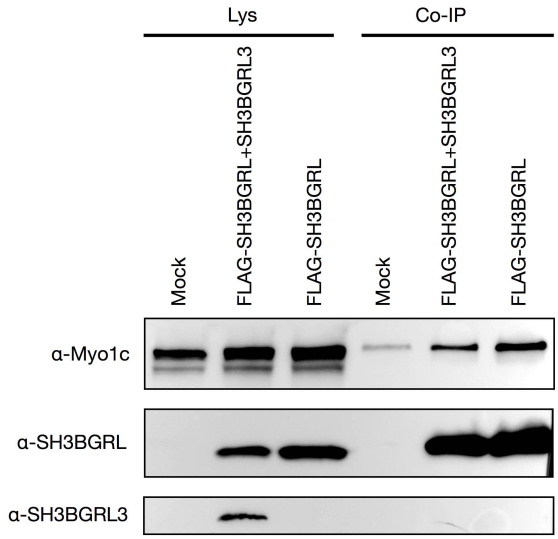

Figure 10. Co-IP using FLAG-SH3BGRL as a bait in SKBR3 cell line. Cells were transfected with pCMV/FLAG (Mock), FLAG-SH3BGRL plus SH3BGRL and FLAG-SH3BGRL only. After Co-IP with anti-FLAG resin and samples run on SDS-PAGE we detected proteins using α-Myo1c, α-SH3BGRL and α-SH3BGRL3 antibodies. Lysates proteins are shown on the right and Co-IP proteins on the left. As we already demonstrated, SH3BGRL is able to Co-IP Myo1c and we revealed that in this complex (SH3BGRL/Myo1c) is not present SH3BGRL3 that is able to Co-IP Myo1c as well but not to bind the Myo1c simultaneously with the SH3BGRL3 protein.

Evaluation of SH3BGRL3, SH3BGRL and Myo1c protein expression in different breast cancer cell line

Founding that SH3BGRL3 and SH3BGRL proteins interact with Myo1c, in SKBR3 cell line, lead us to investigate a possible role of the complex that they form. Since Myo1c is a protein involved in cell membrane and cytoskeleton dynamics, we choose to evaluate SH3BGRL3 and SH3BGRL involvement in cell motility. At first, we choose to silence the SH3BGRL3 and the SH3BGRL expression in order to evaluate their involvement in cell migration and invasion For this purpose, we analysed a proper cellular model that was able to migrate. We checked different breast cancer cell lines (MDA-MB-231, SKBR3, MCF-7, MDA-MB-468, T47D and BT-474) and we found in the highly invasive MDA-MB-231 cell line, a breast cancer cell line derived from a metastatic site [68] which is a typical cell line used for invasiveness experiments, the only one with a high expression of both SH3BGRL3, SH3BGRL and Myo1c (**Figure 11**).

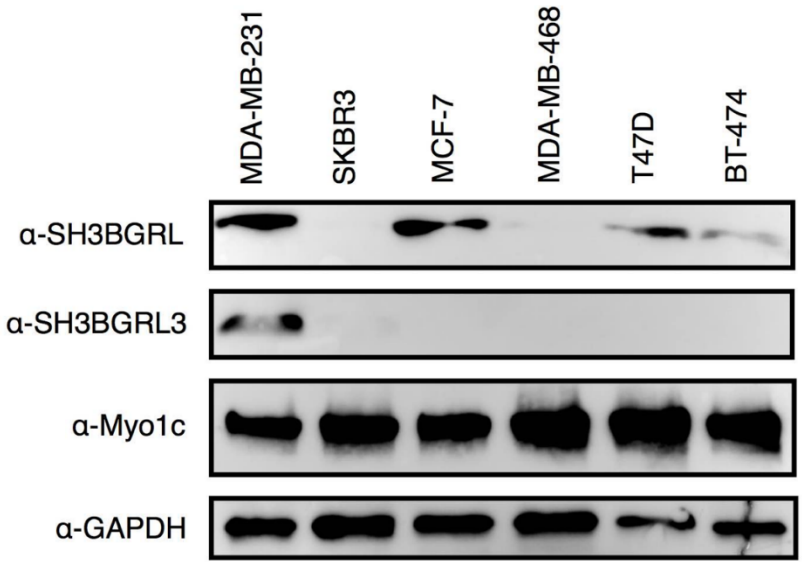

Figure 11. Western blot showing the different expression of SH3BGRL, SH3BGRL3 and Myo1c proteins in MDA-MB-231, SKBR3, MCF-7, MDA-MB-468, T47D and BT-474 breast cancer cell lines. Lysates were collected, run on SDS-PAGE and proteins were detected using α-SH3BGRL, α-SH3BGRL3, α-Myo1c and α-GAPDH (as a control). The highly invasive MDA-MB-231 cell line shows a high expression of both our proteins suggesting it as a good model where to test if a down-expression of SH3BGRL and SH3BGRL3 may impair cell migration and invasiveness in this model.

SH3BGRL3 binds Myo1c in MDA-MB-231 cell line

After having proved the expression of SH3BGRL3 protein in the MDA-MB-231 cell line, we wanted to verify its ability to form intracellular complexes with the Myo1c protein also this cell model. To do this we performed Co-IP experiments as well as co-localization experiments in the MDA-MB-231 model. For the Co-IP, we transiently transfected MDA-MB.231 cells with a specific construct for the expression of the FLAG-SH3BGRL3 fusion protein while a vector for the FLAG expression alone was used as a control, then we incubated the lysates with a FLAG binding resin. We found that also in the highly invasive MDA-MB-231 cell line SH3BGRL3 is able to interact with the Myo1c molecular motor (**Figure 12**), differently from the negative control.

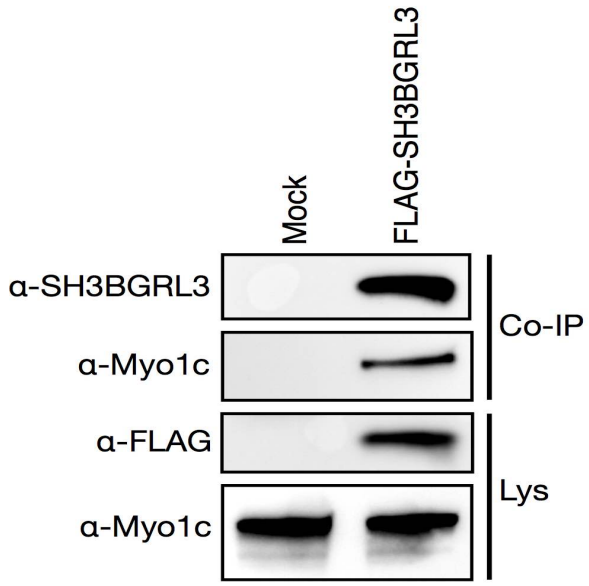

Figure 12. Co-IP of endogenous Myo1c in the MDA-MB-231 cell line after transfection with FLAG-SH3BGRL3 and FLAG alone as a control. After incubation with an anti-FLAG resin, samples were run on SDS-PAGE and proteins were detected by western blot using α-SH3BGRL3, α-Myo1c and α-FLAG antibodies (Co-IP results are shown on the top while lysates are on the bottom).

To validate this data and to identify the localization of SH3BGRL3/Myo1c complexes we performed co-localization experiments by fluorescence assay.

In order to do this, we previously transfected MDA-MB-231 cells by a FLAG-SH3BGRL3 since there was not an α-SH3BGRL3 antibody available for fluorescence staining. We used an antibody α-FLAG (to detect SH3BGRL3 protein) and an α-Myo1c antibody both suitable for fluorescence staining, founding a similar expression pattern of these two proteins as it is shown in **figure 13.A**. Since cellular motility requires the involvement of F-actin [69] we investigated also actin pattern together with SH3BGRL3 and Myo1c, using Phalloidin to stain the actin, determining the distribution of SH3BGRL3, Myo1c and actin in the MDA-MB-231 cell line (**Figure 13.B-C**).

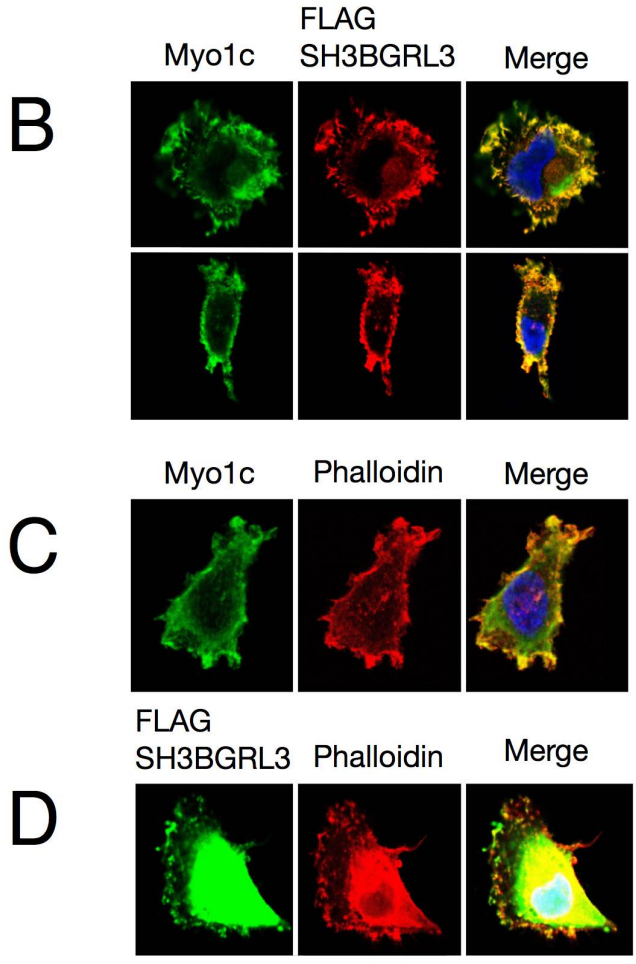

Figure 13.A. Immunofluorescence staining using anti- FLAG antibody (to detect SH3BGRL3 after transfection with FLAG- SH3BGRL3) and anti-Myo1C and Phalloidin (to detect F-actin) on co-localization of Myo1c and SH3BGRL3; **B.** anti-Myo1c and Phalloidin; **C.** SH3BGRL3 and Phalloidin. We report that SH3BGRL3 and Myo1c have a similar distribution pattern and co-localize with actin-enriched structures beneeth the cell membrane.

Our data show that SH3BGRL3 and My1c are proteins that interact together and localize in the same cell membrane areas of actin-enriched structures this may suggest the involvement of these proteins in cell membrane dynamics and/or cell motility.

SH3BGRL3 down-regulation impairs invasion and migration capacity of MDA-MB-231 cell line

After we demonstrated SH3BGRL3 and Myo1c proteins are able to interact, we evaluated the SH3BGRL3 role in cell migration and invasion down-regulating *SH3BGRL3* expression in the MDA-MB-231 cell line by using specific siRNAs against the *SH3BGRL3* gene and using scrambled unspecific siRNA as a negative control. At first, we silenced SH3BGRL3 by two different siRNAs (here called SIRNA^{1} and SIRNA^{2}) as it is shown in **Figure 14.B** and in **Figure 14.C**. We used Boyden chambers for the migration assay which detect the ability of MDA-MB-231 to migrate throw a membrane with specific pores size, while for the invasion assay the same chambers, but covered with Matrigel, have been used to analyse the ability of the cells to digest extracellular matrix, an essential step in the metastatic process (see Materials and Methods). The result of the migration assays, performed with two different siRNAs, shows a statistically significant decrease in the migration capacity of silenced MDA-MB-231 cells respect to the control as is showed in **Figure 14.A**. This data that suggests SH3BGRL3 is as a protein that plays a crucial role in cell migration, according to what Chiang and colleagues have reported [16].

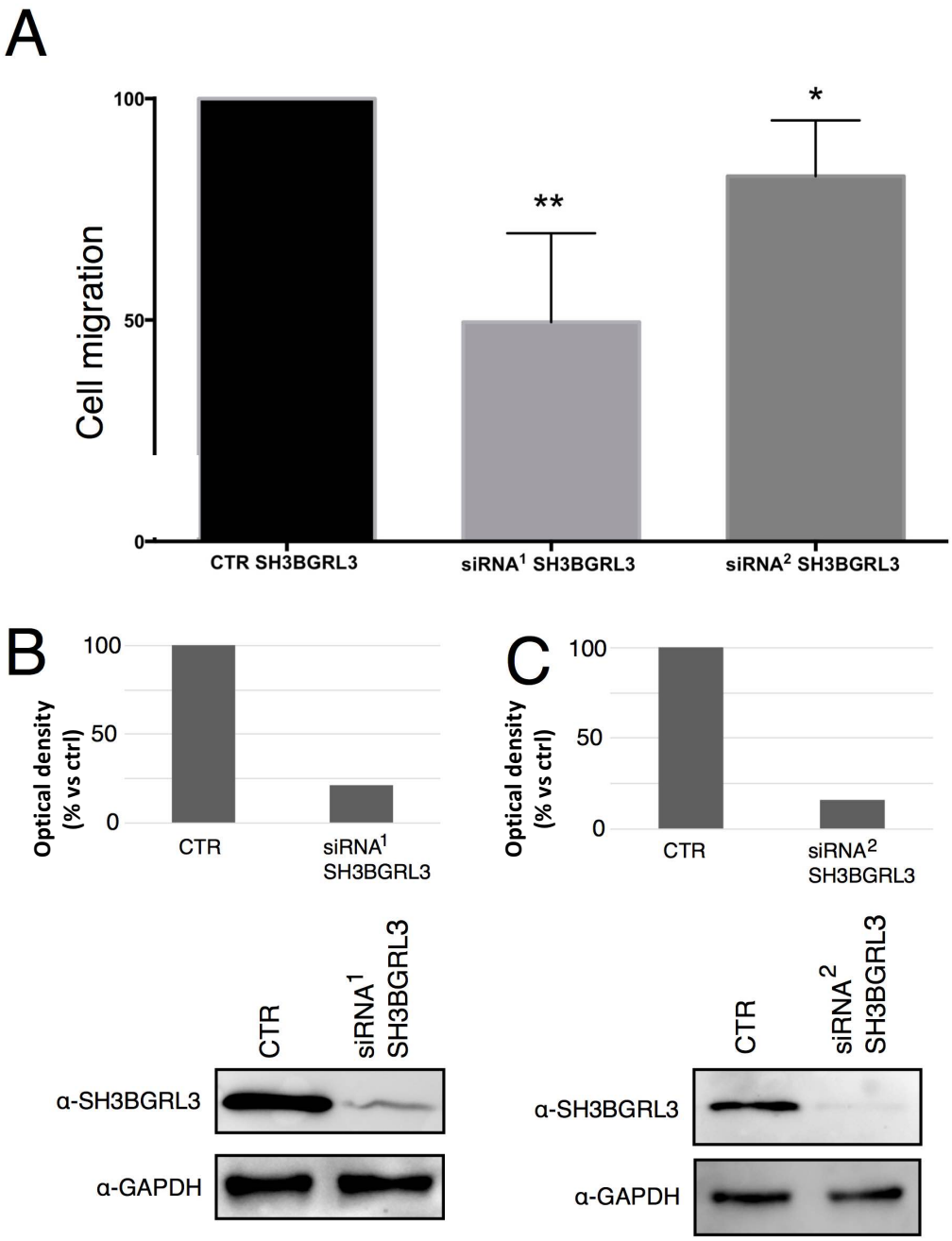

Figure 14. A. This figure shows that the SH3BGRL3 down-regulation decreases, in a statistically significant fashion, the MDA-MB-231 migratory capability, evaluated using Boyden chamber. Pictures were taken on a light microscope from the bottom side of the Transwell membrane and cells were counted after fixation and staining using crystal violet. **B**. and **C**. show the western blot and their relative quantification of SH3BGRL3 silencing by using two different and specific siRNAs. An unspecific scrambled siRNA was used as negative control. Lysate were collected and samples were run on SDS-PAGE and proteins were detected using α-SH3BGRL3 and α-GAPDH as positive control.

In order to evaluate the invasiveness, we performed invasion assay in MDA-MB-231 cell line using Transwells covered with Matrigel to mimic the extracellular matrix, after *SH3BGRL3* silencing by a specific siRNA and an unspecific scrambled siRNAs as a negative control to maintain their motility capacity. Here we show that the SH3BGRL3 down-regulation impairs significantly the invasiveness of MDA-MB-231 cell lines respect to the control (**Figure 15**).

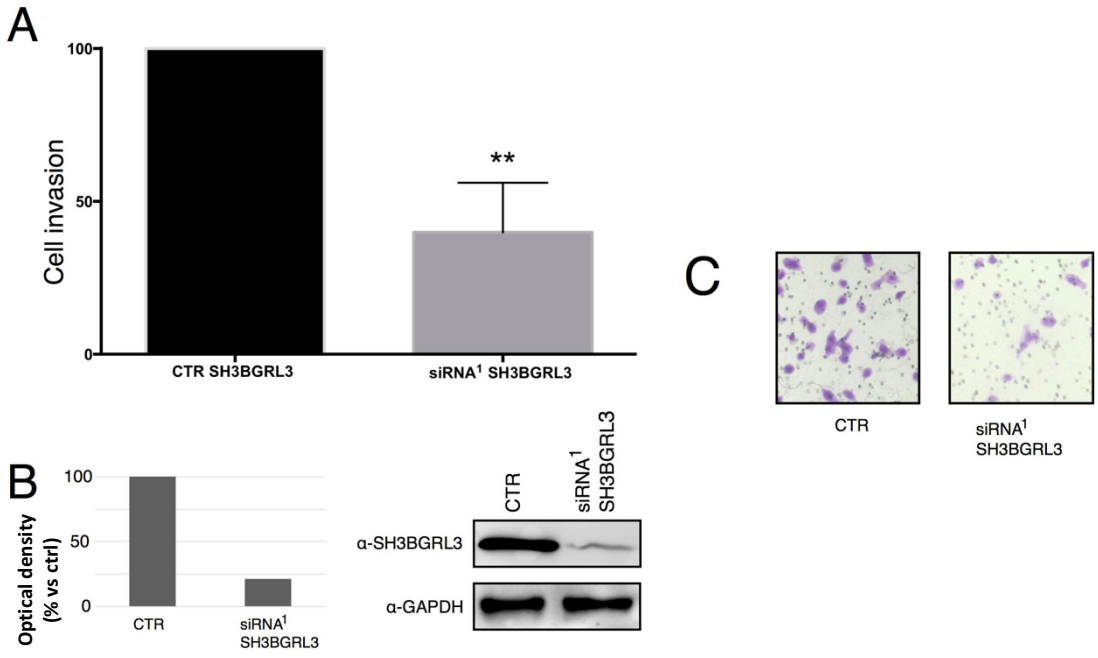

Figure 15. **A**. shows that the SH3BGRL3 down-regulation decreases, in a statistically manner, the MDA-MB-231 invasiveness capability using Transwell chambers covered with Matrigel to analyse the ability of the cells to digest extracellular matrix. **B.** This panel shows the western blot and their relative quantification of SH3BGRL3 after silencing by using a specific siRNA while an unspecific scrambled siRNA was used as negative control. Lysate were collected, samples run on SDS-PAGE and proteins were detected using α-SH3BGRL3 and α-GAPDH as positive control. **C**. Pictures were taken with a light microscope (magnification 10X) from the bottom side of the Transwell membrane and cells were counted after fixation and staining using crystal violet.

The *SH3BGRL3* gene over-expression increases cell motility in MFC-7 cell line

To validate the effect of SH3BGRL3 silencing in cell migration and invasion obtained with the MDA-MB-231 cell line model, we decided to test the cell motility in a different cell line and with a different kind of assay. To do this, we created a stable MCF-7 cell line over-expressing the SH3BGRL3 protein by a specific lentivirus carrying the sequence for *SH3BGRL3* gene and a resistance for puromycin antibiotic (for the selection) while a lentivirus with the only antibiotic resistance was used as a negative control. After the cells had been selected, we verified SH3BGRL3 over-expression by western-blot technique using specific antibodies (**Figure 16.B**). We tested cell migration performing the wound healing assay (Scratch assay) to evaluate specifically the cell motility of SH3BGRL3 over-expressing MCF-7 cells versus control cells and we calculated the wound closure analysing. Pictures were taken at time 0, then 24 hours and 48 hours after the scratch (**Figure 16.C**). According to what we found in MDA-MB-231 cells after the *SH3BGRL3* gene silencing, also in the MCF-7 cells an over-expression of SH3BGRL3 increases cell motility of the lowly invasive MCF-7 cell line (**Figure 16.A**).

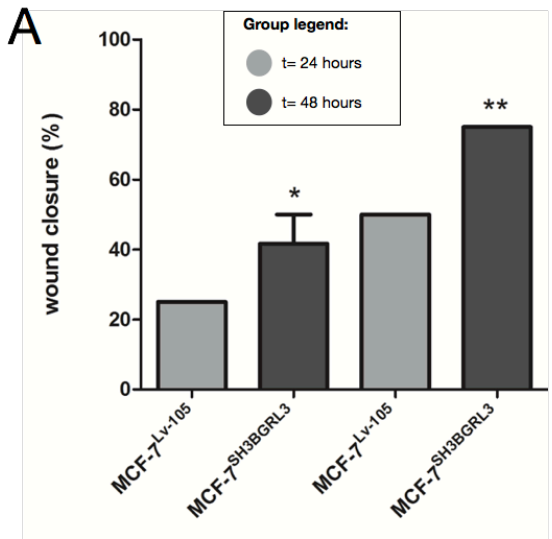

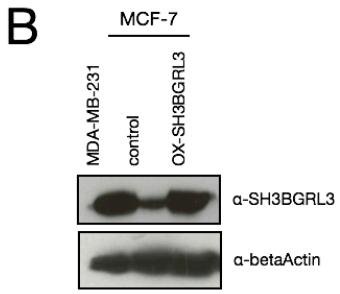

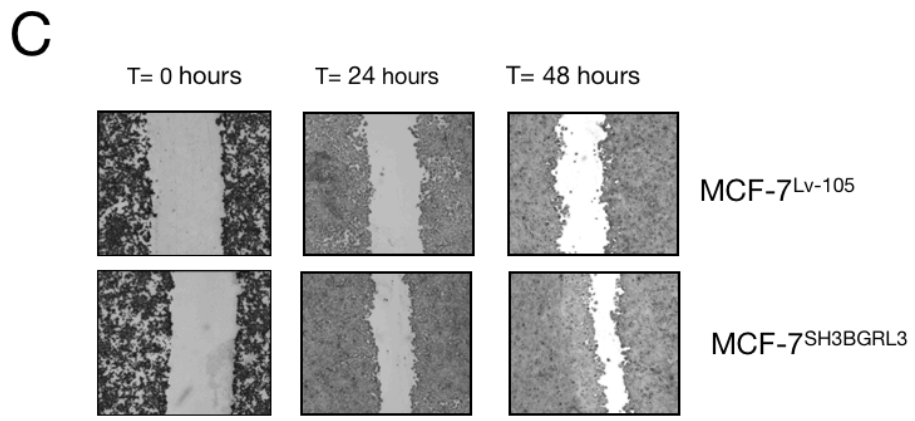

Figure 16 A. SH3BGRL3 over-expression increases cell motility in the SH3BGRL3 over-expressing MCF-7 cell line compared to the control at 24 hours and 48 hours after the scratch. The scratch assay has been performed in a manual way using a 200 μL pippette tip after 12 hours of cell starvation in DMEM without FBS. After the scratch the cells were put in complete medium for 48 hours. The wound closure area was evaluated by imageJ program and the % of the closure was calculate by the formula: *% of wound closure = [(Area$_{t=0h}$- Area$_{t=\Delta h}$)/ Area$_{t=0h}$]x100*. **B**. We evaluated the SH3BGRL3 expression in MDA-MB-231 cells (as a positive control), in MFC-7 control cells (Lv-105) and MCF-7 cells over-expressing the *SH3BGRL3* gene. **C.** Pictures of the wound closure were taken with a light microscope (magnification 10X) at time 0, 24 hours and 48 hours after the scratch.

The *SH3BGRL3* gene over-expression does not affect cell growth/proliferation in MFC-7 cell line

To be sure that the differences observed in the wound closure between the SH3BGRL3 over-expressing MCF-7 cells and control cells were due only by a different cell motility and not by a different on the cell growth, we performed a cell growth assay using the xCELLigence real-time cell analysis (RTCA) system. The SH3BGRL3 over-expression MCF-7 cells and MCF-7 control cells were plated at the same concentration and cell growth was followed for 96 hours after plating. As it is shown in **Figure 17.A**, no difference between in cell growth of SH3BGRL3 over-expressing MCF-7 cells and MCF-7 control cells were observed. In some instance, we evaluated also the cell growth within 48 hours (time range of the scratch assay) without finding any difference between the two samples (**Figure 17.B**) confirming the migration assay.

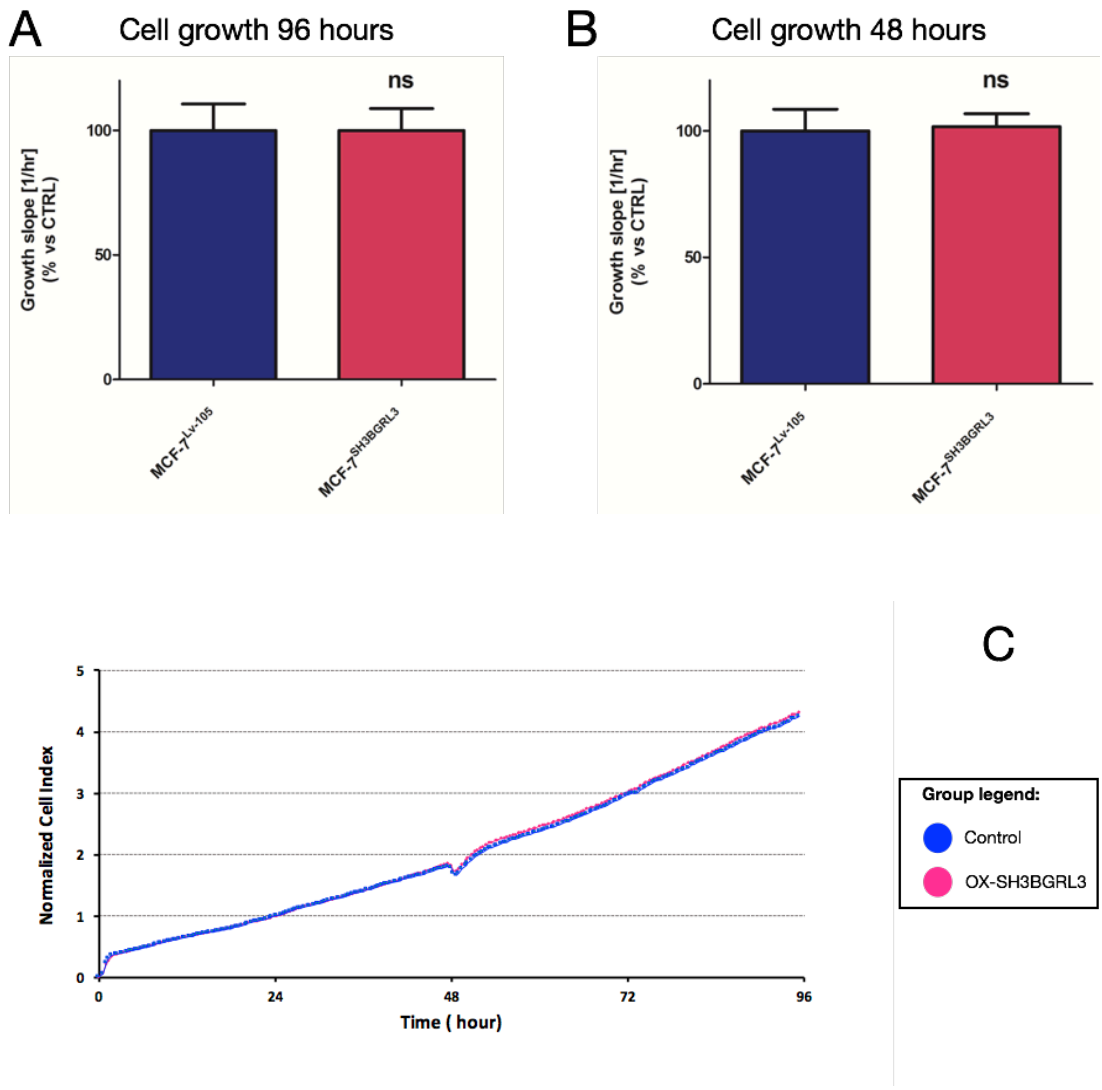

Figure 17. A. Cell growth assay performed by the xCELLigence system real-time cell analysis (RTCA). Cell growth (as a slope inclination of the Cell Index curve in a particular user-defined time range) was evaluated from time 0 to 48 hours after cell plating demonstrating that there is no difference in this time range between MCF-7 control (blue) and MCF-7 SH3BGRL3 over-expressing (pink) assuming that the only difference in the wound closure that we found depends only in differences in cell motility. **B.** Slope cell growth evaluation from 0 hours to 96 hours, no difference was founded neither here. **C**. Normalized cell index curve that show clearly how there is no difference in cell growth between MCF-7 SH3BGRL3 over-expressing and normal MCF-7 cells.

SH3BGRL down-regulation does not affect migration and invasion capacity of MDA-MB-231 cell line

SH3BGRL belongs to the same family of SH3BGRL3 and shows a high homology with it. We demonstrated that also SH3BGRL is able to Co-IP Myo1c in SK-BR-3 cell line [58]. According to this, we performed migration and invasion assays in the highly invasive MDA-MB-231cell line after silencing or not of the *SH3BGRL* gene. As we performed before for SH3BGRL3, we used Boyden chamber to evaluate the migration capability while Transwells covered with Matrigel were used for the invasion assay. We silenced *SH3BGRL* expression by using a specific siRNA directed to its genomic sequence while an unspecific scrambled siRNA was used as a negative control. Differently from what we found in the *SH3BGRL3* silencing experiments, a down-expression of SH3BGRL doesn't impair cell migration (**Figure 18**) and cell invasion (**Figure 18**) in the MDA-MB-231 model.

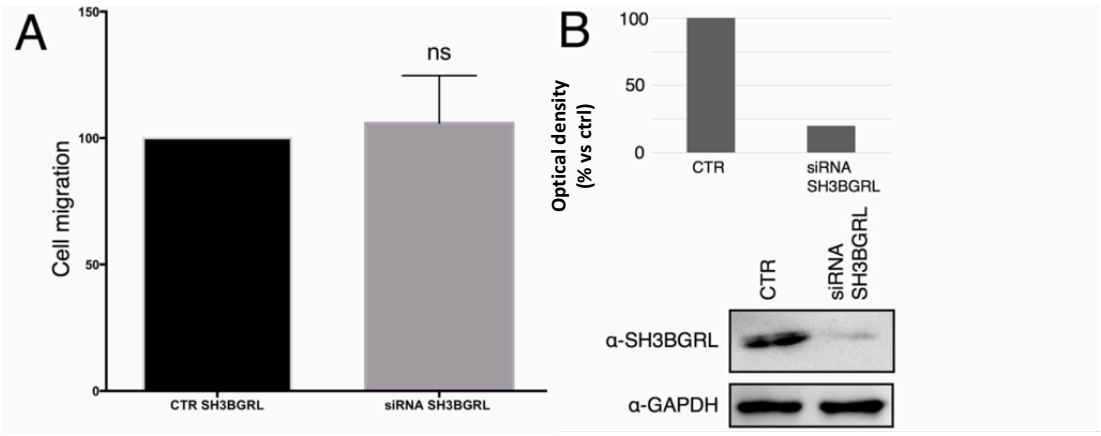

Figure 18 A. Results of the migration assays, after *SH3BGRL* silencing in the MDA-MB-231 cell model, using Boyden chamber. The difference in cells number is not statistically significant Pictures were taken with a light microscope from the bottom side of the Transwell membrane and cells were counted after fixation and staining using crystal violet. **B**. This panel shows the western blot and its relative quantification of *SH3BGRL* silencing by using a specific siRNA while un unspecific scrambled siRNA was used as negative control. Lysate were collected and samples were run on SDS-PAGE and proteins were detected using α-SH3BGRL and α-GAPDH as positive control.

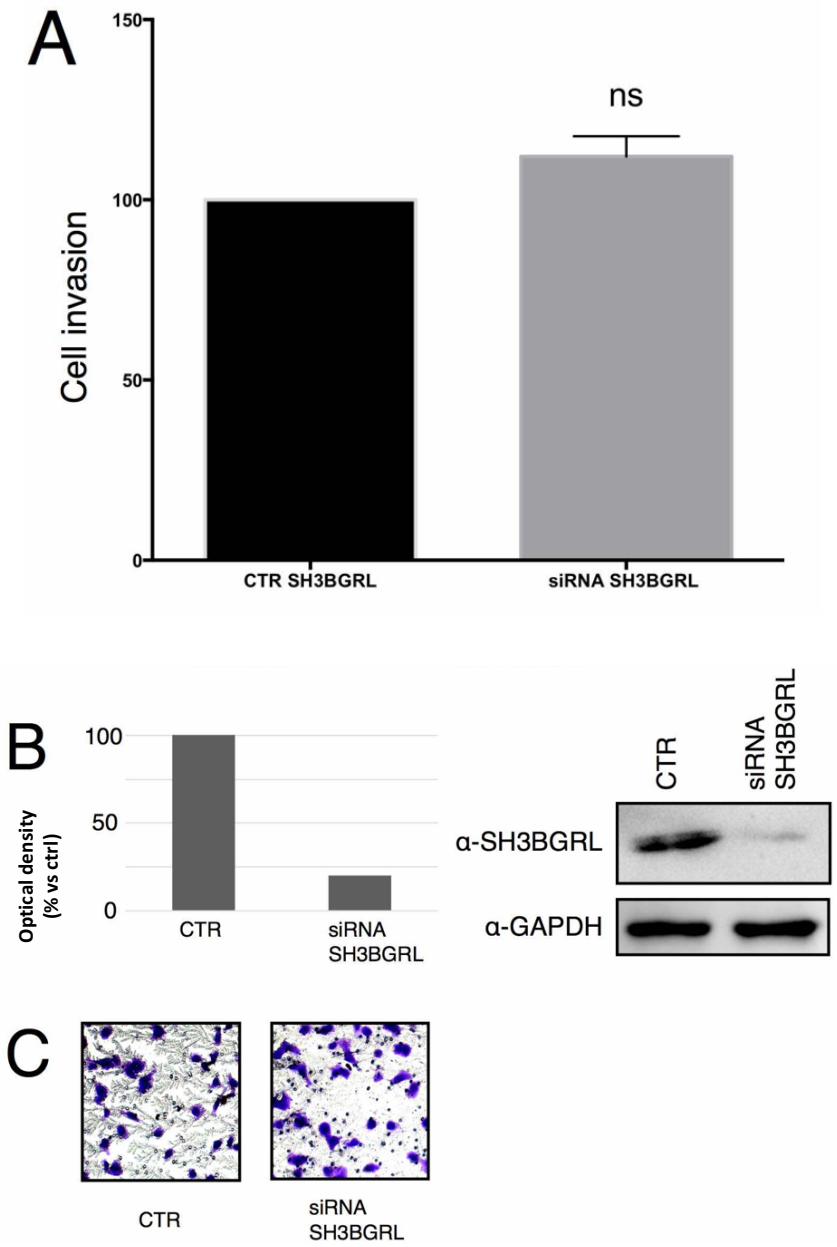

Figure 19 A. Here we show as a SH3BGRL doesn't decreases MDA-MB-231 invasiveness capability either using Transwell chamber covered by Matrigel to analyse the ability of the cell to digest extracellular matrix. **B.** It is shown the western blot and its relative quantification of SH3BGRL silencing by using a specific siRNAs while an unspecific scrambled siRNA was used as negative control. Lysate were collected and samples were run on SDS-PAGE and proteins were detected using α-SH3BGRL and α-GAPDH as positive control. **C**. Pictures were taken on a light microscopy (magnification 10X) from the bottom side of the Transwell membrane and cells were counted after fixation and staining using crystal violet.

SH3BGRL does not Co-IP Myo1c in MDA-MB-231 cell line

Since we didn't find any correlation between SH3BBGRL expression and migration or invasion capability of MDA-MB-231 cell line, we investigated if SH3BGRL were able to form the complex with Myo1c, as SH3BGRL3 does. As we performed before for SH3BGRL3 analysis, we transiently transfected MDA-MB-231 cells with a specific construct for the expression of FLAG-SH3BGRL while a vector for the only FLAG expression was used as a negative control. Subsequently we incubated the lysates with a specific resin binding the FLAG epitope. Despite to what we found for SH3BGRL3, no interaction between SH3BGRL and the Myo1c molecular motor was detected (**Figure 20**). These results can easily explain also the negative results obtained in the migration and invasiveness experiments performed using the MDA-MB-231 cell line.

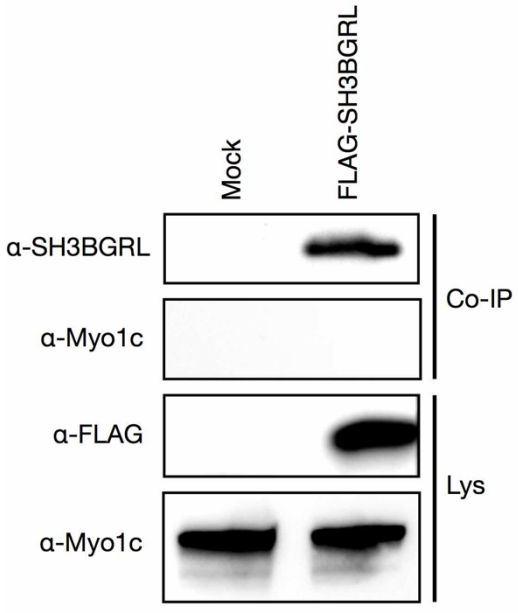

Figure 20. Co-IP of endogenous Myo1c in MDA-MB-231 cells after transfection with FLAG-SH3BGRL and FLAG alone as a control. No Myo1c was Co-IP by SH3BGRL. After incubation with an anti-FLAG resin, samples were run on SDS-PAGE and proteins were detected by western blotting using α-SH3BGRL, α-Myo1c and α-FLAG antibodies (Co-IP results are shown on the top while lysates are on the bottom).

No interaction between SH3BGRL3 or SH3BGRL with ERBb2, EGFR and Grb2 were founded

As already said, a published paper showed that SH3BGRL (or SH3BGRL3) was able to binds ErbB1 (EGFR) at the phosphorylated tyrosine Y_{891} and ErbB2 at phosphorylated Y_{923} and Y_{1196} by proteomyc analysis [54]. We performed Co-IP experiments to validate this. At first, we transiently transfected SKBR3 cell line with FLAG-SH3BGRL3 and FLAG only as negative control and we tried to Co-IP ErbB2 by using an anti-FLAG resin. Since this result was negative we tried te reversed Co-IP (using ErbB2 as bait) that was negative too (data not shown), thus we assumed that there was no interaction between SH3BGRL3 and ErbB2 receptor. Recently, accordingly to data reported by Chiang and collegueas that found SH3BGR3 positively associated with higher histologic grading and muscle invasiveness of urothelial carcinoma and able to interact with phosphor-EGFR at Y1068, Y1086, and Y1173 through Grb2 by its proline-rich motif and activates the Akt-associated signalling pathway [23] we were interested to investigate the interaction between SH3BGRL3 and Grb2 also in MDA-MB-231 cell line we already correlated SH3BGRL3 function with the cell migration and invasion. Since we didn't find that SH3BGRL3 could to Co-immunoprecipitate phosphor-EGFR after transiently transfection of MDA-MB-231 cells with FLAG-SH3BGRL3 and after EGFR treatment (data not shown), we tried then to demonstrate the interaction between SH3BGRL3 and ErbB2 in SKBR3 cells through Grb2 adaptor protein. For this purpose, we transiently transfected SKBR3 cell line with FLAG-SH3BGRL3 and FLAG alone as negative control. We incubated cell lysates with an anti-FLAG resin and we detected proteins by WB. **Figure 21** shows that no interaction between SH3BGRL3 (or SH3BGRL) and Grb2 proteins was found. Of note, SH3BGRL3 protein e doesn't present a usual SH3-binding domain that can interact with Grb2.

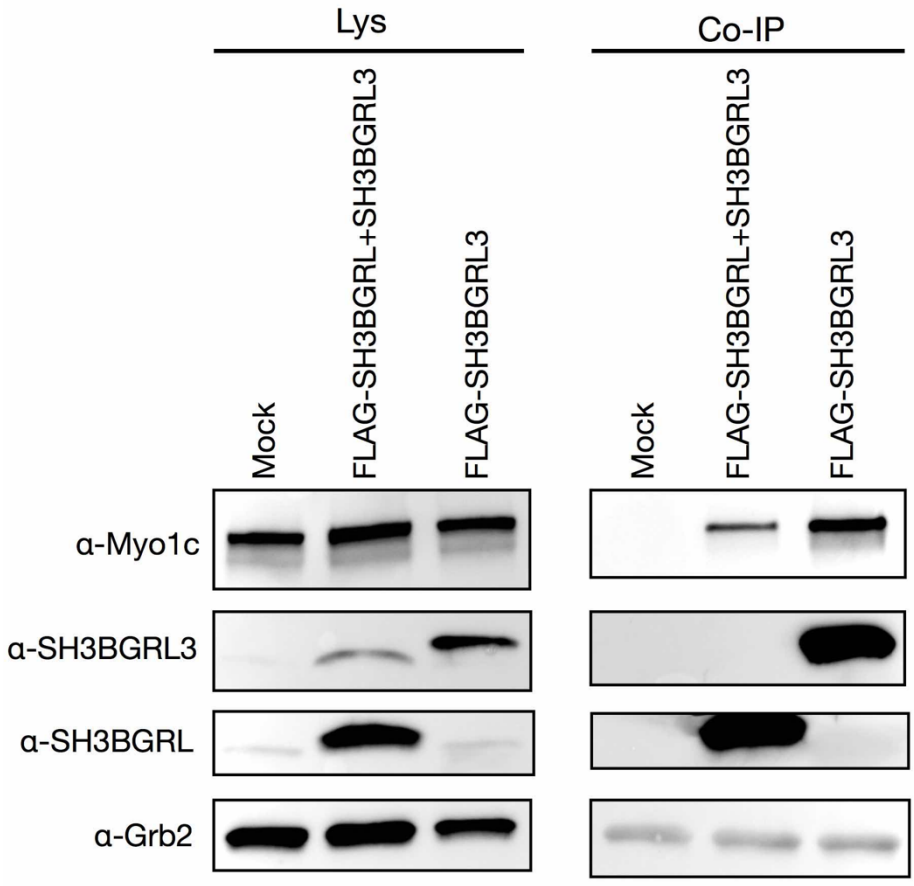

Figure 21. Grb2 Co-IP using SH3BGRL3 or SH3BGRL as a bait, no interaction was founded in SKBR3 cell line lysates. We used Myo1c Co-IP as positive control. Cells were transiently transfected with constructs coding for FLAG-SH3BGRL (and SH3BGRL3), FLAG-SH3BGRL3 alone or FLAG alone as negative control. Lysates (on the left) were incubates with an anti-FLAG resin, run on SDS-page and blotted proteins band were detected on WB using α-Myo1c, α-SH3BGRL3, α-SH3BGRL and α-Myo1c antibodies. Co-IP results are shown on the right.

SH3BGRL3 is a cytosolic protein that is not found in the mitochondrial fraction

To further lighten the SH3BGRL3 function and its involvement in cell motility we invastigated the presence of the SH3BGRL3 protein in isolated mitochondria purified from MDA-MB-231 cells. We decided to investigate the presence of SH3BGRL3 in mitochondria since is been reported recently in the litterature how mitochondrial dynamics regulates migration and invasion of breast cancer cell [70]. Mitochondria are organelles that provide the majority of the energy in most cells. Since mitochondria balance is maintained by two

opposing processes called fission and fusion, in cancer cells dysfunction of mitochondria has been implicated in processes involved in tumorigenesis such as metastasis [71]. Cancer cells exhibited an excess of mitochondrial fission and impaired mitochondrial fusion that are involved in breast cancer cell migration and invasion (e.g. MDA-MB-231). In breast cancer cells, also lamellipodia formation depends on the mitochondria dynamics. According to this we isolated mitochondria from MDA-MB-231 cells and after mitochondria lysis we analysed the expression of SH3BGRL3 by western blot. No SH3BGRL3 signal was founded in isolated mitochondria (**Figure 22**), suggesting that SH3BGRL3 is a cytosolic protein that does not belonging to the mitochondrial fraction.

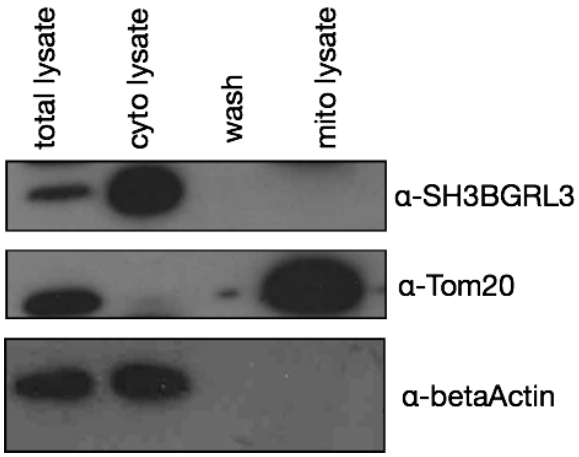

Figure 22. Analysis of SH3BGRL3 presence in isolated mitochondria by western blot. SH3BGRL3 was not found in mitochondria isolated from MDA-MB-231 breast cancer cell line. We used α-betaActin as a cytoplasmatic marker and α-Tom20 as a mitochondrial marker.

Myo1c as a novel exosomal marker of microvescicles isolated from the highly invasive MDA-MB-231 cell line

According to what recent reported papers about the presence of SH3BGRL3 in the secretome or urine of patients with different types of tumor (e.g. urothelial carcinoma, papillary thyroid carcinoma, lung adenocarcinoma), data that suggests SH3BGRL3 as an extracellular protein associated with a higher histologic grading and muscle invasiveness of these type of tumor [23], we investigated the presence of SH3BGRL3 in the microvesicle population secreted by the highly invasive MDA-MB-231 cell line. After media ultracentrifugation, microvesiscles were lysated and protein were detected by western blot technique using α-Alix (as an exosomal marker), α-Myo1c (as an intracellular marker), α-SH3BGRL and α-SH3BGRL3 antibodies. We didn't find SH3BGRL3 protein as well as SH3BGRL protein in the microvesicle lysates but a clear band was found for the Myo1c (**Figure 23**) suggesting this protein as a possible novel exosomal marker. Since Myo1c is a protein able to interact with actin-cytoskeleton and the cell membrane, it sounds possible that it may be involved in microvescicles formation and in their movement to the plasma membrane for the secretion in the outside environment.

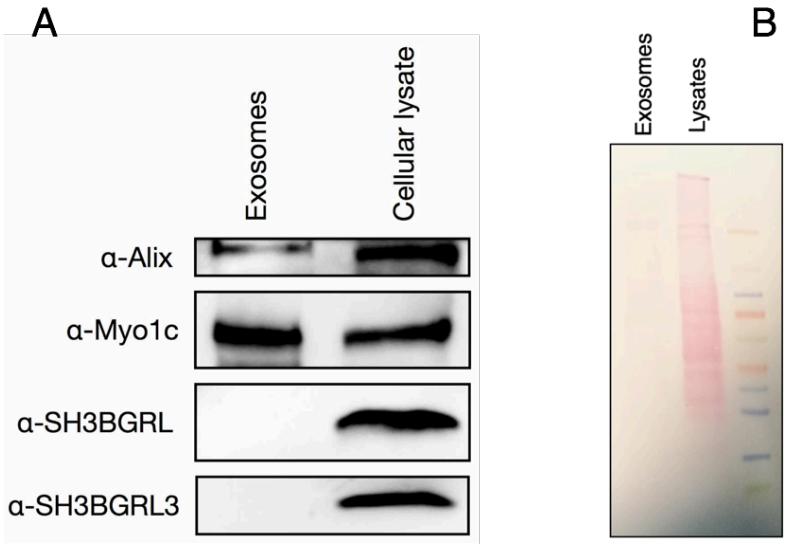

Figure 23. A. Microvesicles isolation from MDA-MB-231 cells. Conditioned media was collected after 72h of incubation and centrifuged at different speeds to remove dead cells, cell

debris and macrovesicles. The micovesicles pellet was lysed and protein were detected by western blot analysis using α-Alix (as a specific exosomal marker), α-Myo1c (as an intracellular marker), α-SH3BGRL and α-SH3BGRL3 antibodies. No SH3BGRL3 and SH3BGRL signal were detected. We founded Myo1c enrichment in exosomal lysate suggesting it as a new potential marker of exosomes isolated from MDA-MB-231 cell line. Exosomal lysate is shown on the left and cellular lysate on the right. **B.** Western blotting membrane after red pounceau staining. Though exosome proteins are less than cellular lysates, the total amount of Myo1c in exosomes reveals these microvesicles to be enriched in Myo1c.

SH3BGRL3 increases cell metabolism in the SH3BGRL3 over-expressing MCF-7 cells

A cell that migrates and spreads into different part of the organism requires lots of energy in order to satisfy all the changes in cytoskeleton/plasma membrane rearrangements (e.g. formation of lamellipodia, psedudopodia or fillipodia), the capability to digest the extra-cellular matrix (invasion) and the synthesis and secretion of new proteins [73]. For this reason, we evaluated the metabolism (glycolysis and mitochondria respiration) of the SH3BGRL3 over-expressing MCF-7 cells compared to control MCF-7 cells by analysing the metabolic flux with the Seahorse XFe96. Interestingly, **Figure 24** illustrates that the SH3BGRL3 over-expressing MCF-7 cells show a large increase in the oxygen consumption rates (OCR) compared to control MCF-7 cells, processed in parallel. Also glycolysis was increased, as measured by the ECAR (extracellular acidification rate) (**Figure 25**). By these results the SH3BGRL3 over-expressing MCF-7 cells seem to be more glycolytic and shown an increase also in the OCR compared to the control MCF-7 cells.

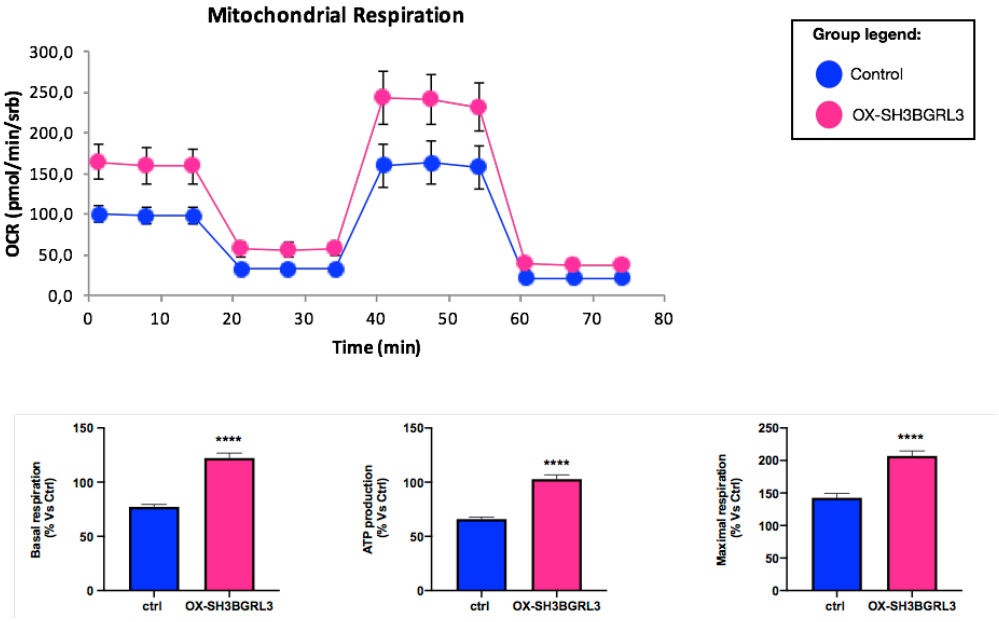

Figure 24. SH3BGRL3 increases mitochondrial respiration in the SH3BGRL3 over-expressing MCF-7 cells. The metabolic profile of MCF-7 monolayers was assessed using the Seahorse XFe96 analyzer. At the top is shown a representative tracing of metabolic flux, at the bottom is reported a significant increase in basal respiration, proton leak and maximal respiration of SH3BGRL3 over-expressing MCF-7 cells (pink) compared to MCF-7 control cells (blue).

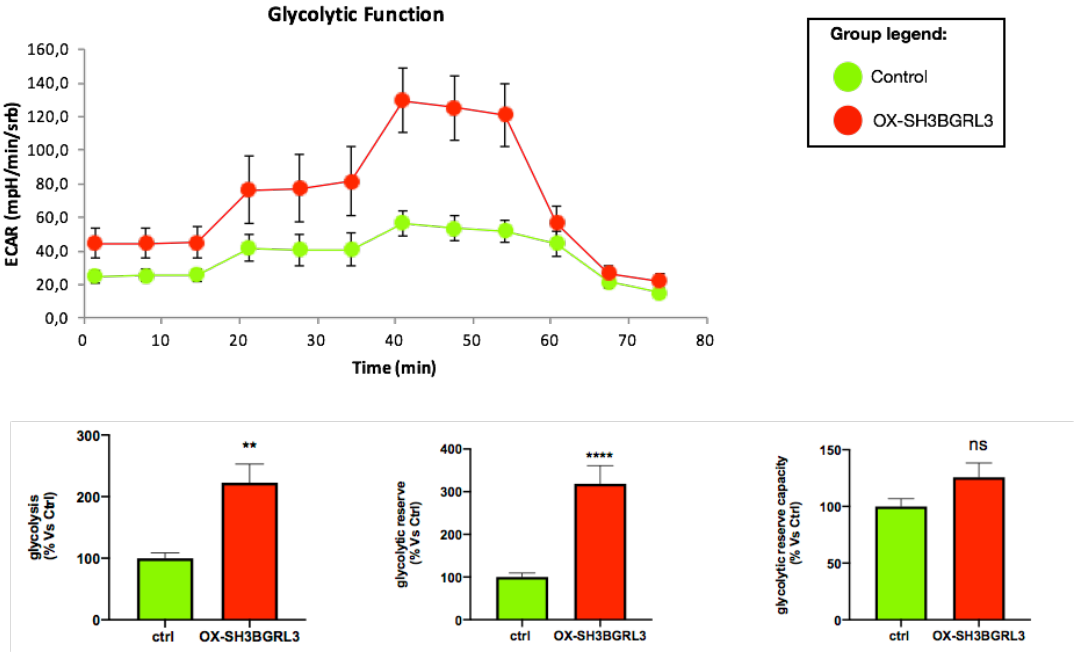

Figure 25. Glycolysis is increased in the SH3BGRL3 over-expressing MCF-7 cells.

The metabolic profile of MCF-7 monolayers was assessed using the Seahorse XF-e96 analyzer. At the top is shown a representative tracing of metabolic flux, at the bottom the analysis of the samples shown an increase in glycolysis, glycolytic reserve and glycolytic reserve capacity as well of the SH3BGRL3 over-expressing MCF-7 cells (red) compared to MCF-7 control cells (green).

The SH3BGRL3 protein is not related to cell "stemness" performing mammosphere assay

As migration and invasion are required for metastasis we were interested to evaluate if SH3BGRL3 is also involved in the cancer stem cell maintenance as a new potential stemness marker. To do this, we compared the SH3BGRL3 over-expressing MCF-7 cells to control MCF-7 cells performing mammosphere assay. **Figure 26** shows that no significantly differences in mammospheres formation were founded between SH3BGRL3 over-expressing MFC-7 cells and MCF-7 control cells. This result suggests that the SH3BGRL3 protein is not involved in "stemness" property of the cell though both cell motility and "stemness" take part in the metastatic process [74].

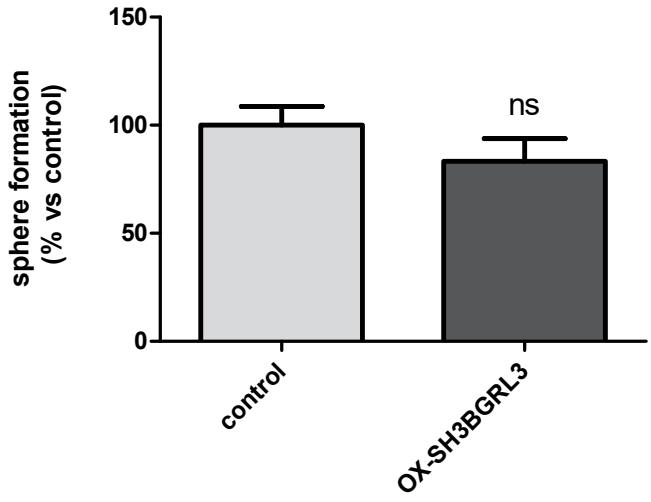

Figure 26. Mammosphere formation in the SH3BGRL3 over-expressing MCF-7 cells versus control MCF-7 cells. The result shows as no differences were founded between the samples. Evaluation of mammosphere formation in the SH3BGRL3 over-expressing MCF-7 cells and

control MCF7 cells cultured in low attachment plates for 5 days before counting. The data shown are the mean ± SEM of 3 independent experiments performed in triplicate. $p < 0.05$.

SH3BGRL3 implicates Estrogen Receptor-alpha downregulation and the resistance to 4'OH-Tamoxifen in SH3BGRL3 over-expressing MCF-7 cells

It has been recently reported in the literature a possible correlation between the SH3BGRL3 protein and the Estrogen Receptor-alpha (ERα) expression. Since ERα silencing in MCF-7 cells induces several markers expression of the Epithelial-Mesenchymal Transition (EMT), the expression of EGFR and HER2 receptors that increases cell proliferation, migration and invasion [74] and un up-regulation of the *SH3BGRL3* gene expression in MCF-7 breast cancer [75] we decided to evaluate ERα expression in our model. We found a statistically significant reduction of the ERα expression in the SH3BGRL3 over-expressing MCF-7 cells compared to control MCF-7 cells (**figure 26.A**). This data suggests that *SH3BGRL3* expression may be under ERα control, since its expression in down-regulated in ERα-positive breast cancer cell lines [76], considering that ERα is a transcription factor composed of domains able to bind the DNA to activate/repress the transcription of different genes [77]. It's also interesting how the treatment with a combination of Estradiol (E_2) and 4'OH-Tamoxifen (4'OH-Tam), an active metabolite of Tamoxifen, significantly promotes cells motility on MCF-7 cell line [78]. Accordingly, we evaluated 4'OH-Tam effect on the SH3BGRL3 over-expressing MCF-7 cells performing cell growth assays using the xCELLigence RTCA system. Since 4'OH-Tam is a partial agonist of estrogen receptors used for the treatment of estrogen receptor-positive (ER+) breast cancer [79,80] and its action in possible only on cancer ER-positive cells and not on ER-negative (e.g. MDA-MB-231), choose to investigate if theSH3BGRL3 over-expressing MCF-7 cells, that we found to show a reduction of ERα expression, ,may be resistant to 4'OH-Tam.

24 hours after cells plating, we treated them with 4'OH-Tam [1μM] for 200 hours and we observed that the SH3BGRL3 over-expressing MCF-7 cell, that exhibit an ERα down-regulation expression, are more resistant to 4'OH-Tam compared to control MCF-7 cells (**Figure 27**).

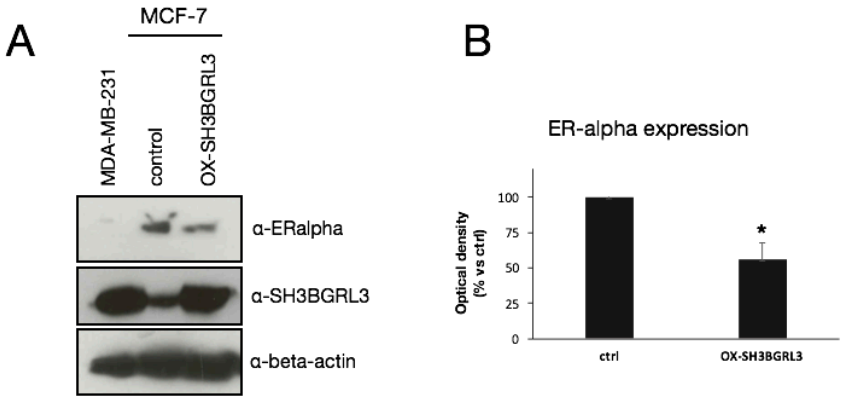

Figure 26. **A** Western blot analysis of ERα expression in the SH3BGRL3 over-expressing MCF-7 cells compared to control MCF-7 (Lv-105) cells. MDA-MB-231 cell lysate (right) was used as a positive control for SH3BGRL3 expression and as a negative one for ERα expression (ER-negative cell line).

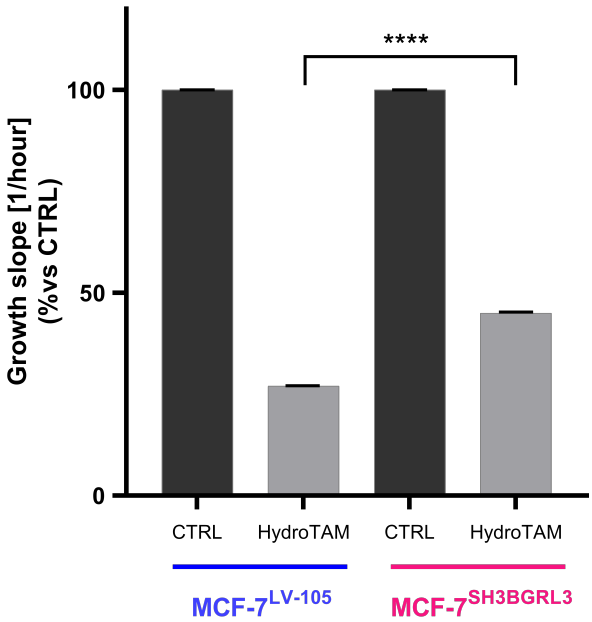

Figure 27. Cell growth assay performed by xCELLigence system real-time cell analysis (RTCA). The cells were treated with 4'OH-Tam (4-hydroxytamoxifen) 24 hours (time point of normalization) after plating and cell growth (as a slope inclination of the Cell Index curve in a

particular user-defined time range) was evaluated between 150 hours and 200 hours to appreciate any difference since 4'OH-Tam is a cytostatic drug. Media and 4'OH-Tam were changed every 48 hours. Comparing the slope (% vs CTRL) of the SH3BGRL3 over-expressing MCF-7 cells to control MCF-7 cells we found a statistically significant increasing of cell growth in the SH3BGRL3 over-expressing MCF-7 cells after 4'-OH treatment respect to the control (treated with the only vehicle).

DISCUSSION

The aim of this project was to characterize the proteins belonging to the SH3BGR family, in particular we focused our study on the SH3BGRL and SH3BGRL3 proteins.

After we found SH3BGRL3 and SH3BGRL proteins able to interact with the molecular motor Myo1c, more specifically SH3BGRL3 protein binds the Myo1c IQ domains, in SKBR3 breast cancer cell line [58], we wanted to investigate if Ca^{2+} could play a role in the SH3BGRL3/Myo1c complex formation since CaM is able to bind IQ domains in a low Ca^{2+} concentration [81]. We found that SH3BGRL3 protein binds Myo1c only in the presence of Ca^{2+}, while this binding doesn't occur in the presence of a Ca^{2+} chelator (e.g. EGTA). This suggests that SH3BGRL3 and CaM are two proteins that both bind Myo1c IQ domains but at different Ca^{2+} concentration, suggesting Ca^{2+}-driven changes in the "neck" region of the Myo1c and this may modulate the Myo1c function based on Ca^{2+} concentration inside the cells.

Since we previously demonstrated that both SH3BGRL and SH3BGRL3 proteins are able to Co-IP Myo1c in SKBR3 model [58], we investigated if SH3BGRL and SH3BGRL3 may be simultaneously present in the complex with the Myo1C. Accordingly, we co-transfected the SKBR3 cell line with both SH3BGRL and SH3BGRL3 using SH3BGRL as a bait: we found that Myo1c co-immunoprecipitates whereas SH3BGRL3 doesn't, indicating that the binding of SH3BGRL and SH3BGRL3 with Myo1c is mutually exclusive and this could suggest a different role between SH3BGRL and SH3BGRL3 proteins.

Since we have never succeeded to demonstrate any interaction between SH3BGRL3 (or SH3BGRL) with ErbB1 (or EGFR) and ErbB2, differently from what is reported in different studies [26, 55], we investigated the interaction

between the Grb2 adaptor protein and SH3BGRL3. We choose Grb2 because we though it could be the link between SH3BGRL3 and EGF-Receptors, since SH3BGRL3 lacks of the SH3-binding domain necessary to interact with the phosphorylated tyrosine of ErbB1 or ErbB2 [55]. Also in this way, no interaction between the SH3BGRL3 (or SH3BGRL) protein and Grb2 has been founded.

Subsequently, we focused our experiments to investigate any possible function correlated to the SH3BGRL3 (or SH3BGRL)/Myo1c protein complex. Myo1c has multiple and different functions inside the cells and our results suggest SH3BGRL3 as a possible candidate in Myo1c regulation through its interaction via IQ domains. Since Chang and colleagues [26] found SH3BGRL3 in the urine of patients with urothelial carcinoma, an up-regulation in primary bladder cancer cells and its involvement in cancer cell proliferation, epithelial-mesenchymal transition (EMT) and cell migration, we decided to investigate the SH3BGRL3 role in cell migration and invasion that are both essential steps in cancer metastasis [82]. For this reason, we performed migration and invasion assays after SH3BGRL3 (or SH3BGRL) down-regulation. At first, it was necessary to find another cell model (different from the SKBR3 cell line) and we found in the highly invasive MDA-MB-231 cell line a good model since these cells expressed both SH3BGRL3 and Myo1c proteins and form the complex together (verified by Co-immunoprecipitation and Co-localization experiments).

Our data shows a decrease in migration and invasion capability of the MDA-MB-231 cells when *SH3BGRL*3 gene in down-regulated, confirming what Chang and colleagues have been reported in their paper [26].

According to our data attended in the SKBR3 cell line, we also evaluated the SH3BGRL role in cell migration and invasion. Differently from SH3BGRL3, the *SH3BGRL* gene down-regulation doesn't compromise MDA-MB-231 migration and invasion capability. As expected, Co-immunoprecipitation experiments were not able to demonstrate the SH3BGRL/Myo1c complex formation in the MDA-MB-231 cell line.

We are not able to explain this particular Myo1c behavior on its capacity to bind or not SH3BGRL protein among two different cell lines but we found in literature a similar behavior of the Myo1c protein on the binding with SHIP2 interactor participating in the control of cell migration in 1321 N1 glioblastoma cells but not in COS-7 cell line [83].

To confirm our data about the SH3BGRL3 protein involvement in cell migration, we created a MCF-7 cell line stably over-expressing for the *SH3BGRL3* gene. Using the scratch assay, we found an increase in the motility capability of this cell line. Since we didn't find any difference in the cell growth, performing cell growth assays, as Chang et al. reported [26], we suggest SH3BGRL3 as a protein involved in the cell motility and not in the cell proliferation.

Since a few recent papers [23, 24, 25, 26] suggested that SH3BGRL3 could be also secreted, and since secreted proteins are necessary for the cells invasiveness (e.g. metalloproteinase that are able to digest the Extracellular Matrix) and microvesicles like exosomes contain different molecules (proteins, lipids and nuclei acids) able to modify phenotype of normal target cell into a cancer one [84, 85], we isolated exosomes from MDA-MB-231 to investigate any SH3BGRL3 involvement in the microvesicles system but we didn't find any SH3BGRL3 expression in exosomes secreted by the MDA-MB-231 cell line. Otherwise, a high amount of Myo1c has been founded suggesting Myo1c as a new microvesicles marker for the characterization of isolated exosomes from MDA-MB-231 cell line.

Since during the metastatic process cancer cells require to preserve their "stemness" properties [86], we investigate SH3BGRL3 role in cell "stemness" performing a mammospheres assay that showed no correlation between SH3BGRL3 over-expressing MCF-7 cells and the ability of the cells to growth and proliferate in non-adherens conditions. Interestingly, we found an increase on the metabolic profile of the SH3BGRL3 over-expressing MFC-7 cells

respect to control MCF-7 cells based on oxygen consumption rate (OCR) and extracellular acidification rate (ECAR) suggesting that these cells require a large amount of energy. We can explain these data looking at our results about the migration, cells able to migrate requires high level of ATP production to satisfy the cytoskeleton changes and plasma membrane remodelling during this process [87].

Recently, different studies have been reported an interesting correlation between Estrogen-Receptor Alpha (ERα) and SH3BGRL3 expression. It seems that ERα works as suppressor of *SH3BGRL3* gene expression and that perhaps may explain the higher SH3BGRL3 protein amount in MDA-MB-231 cell line (Estrogen-ReceptorAlpha negative) respect to the lower SH3BGRL3 expression in MCF-7 cell line (Estrogen-Receptor positive) [76, 77, 78, 79, 80]. This can also explain the different ability to migrate between MDA-MB-231 and MCF- 7 cell lines [68] considering that ERα expression controls cell migration, stemness and EMT process [88]. According to these data and the literature, we found in the SH3BGRL3 over-expressing MCF-7 cells an increase of migration ability through scratch assay, a significant reduction on the ERα expression and we also demonstrated these cells to be more resistant to the 4'OH-Tam treatment respect to control MCF-7.

In the final analysis, our work and the poor literature about the SH3BGR family suggests that these proteins can have an important role in aggressiveness and metastasis development of different type of tumors.

CONCLUSIONS AND OBSERVATIONS OF THE THESIS

SH3-Domain **B**inding **G**lutamic acid **R**ich **L**ike **3** (SH3BGRL3) protein has enrolled as a potential tumorigenic protein through specific interactions with others proteins. In our work, we found that Co-IP could not confirm the interaction between SH3BGRL3 (or SH3BGRL) and ErBb2/EGFR/Grb2.

In addition, our results confirm the interaction of Myo1c with SH3BGRL3 in SKBR3 and MDA-MB-231 breast cancer cell linesci which does not occur with SH3BGRL protein in the MDA-MB-231 model.

Our functional studies further included that:

SH3BGRL3/Myo1c complex formation is Ca^{2+}-dependent;

SH3BGRL3 AND Myo1c localise to the actin-enriched membrane area supporting their involvement in cell membrane and cytoskeleton dynamics;

There is a detectable expression difference among SH3BGRL and SH3BGRL3 proteins in breast cancer cell lines. Moreover, the expression of SH3BGRL3 seems to be characteristic in the Triple Negative Breas Cancer (TNBC) cell lines;

Inhibited SH3BGRL3 expression impairs migration/invasion capability of TNBC cell line (e.g. MDA-MB-231);

Over-expressing SH3BGRL3 increases cell motility and tamoxifen resistance without influencing the baseline proliferation of ER^+ cell line that are originally SH3BGRL3 negative (e.g. MCF-7).

In parallel, we found another interesting observation from SH3BGRL3 exosome expression study that Myo1c could be e potential microvesicle marker.

Based on these, the SH3BGRL3 protein could influence cell motility, cell invasiveness, and it could be involved in therapy resistance of breast cancer.

BIBLIOGRAPHY

1. Scartezzini P, Egeo A, Colella S, Fumagalli P, Arrigo P, et al. Cloning a new human gene from chromosome 21q22.3 encoding a glutamic acid-rich protein expressed in heart and skeletal muscle. Hum Genet. 1997;99:387-392.

2. Egeo A, Di Lisi1 R, Sandri C, Mazzocco M, Lapide M, et al. Developmental expression of the SH3BGR gene, mapping to the Down syndrome heart critical region. Mech Dev. 2000;90:313-316.

3. Claudia Sandri, Raffaella Di Lisi, Anne Picard, Carla Argentini, Elisa Calabria, Kristene Myklak, Paolo Scartezzini, Stefano Schiaffino. Heart morphogenesis is not affected by overexpression of the Sh3bgr gene mapping to the Down syndrome heart critical region. Hum Genet (2004) 114 : 517–519 DOI 10.1007/s00439-004-1088-8.

4. Natalya Kurochkina & Udayan Guha. SH3 domains: modules of protein–protein interactions. Biophys Rev (2013) 5:29–39 DOI 10.1007/s12551-012-0081-z.

5. Jutta Beneken, Jian Cheng, TuBo Xiao, Mutsuo Nuriya, Joseph P. Yuan, Paul F. Worley, Daniel J. Leahy. Structure of the Homer EVH1 Domain-Peptide ComplexReveals a New Twist in Polyproline Recognition. Neuron, Vol. 26, 143–154, April, 2000, Copyright 2000 by Cell Press.

6. Jang DG, Sim HJ, Song EK, Medina-Ruiz S, Seo JK, Park TJ. A thioredoxin fold protein Sh3bgr regulates Enah and is necessary for proper sarcomere formation. Dev Biol. 2015;405:1-9.

8. Gabriele Assenza, Camillo Autore, Bruno Marino. Hypertrophic cardiomyopathy in a patient with Down's syndrome. Journal of Cardiovascular Medicine. 8(6):463–464.

7. N.A. Bearda, D.R. Laverb, A.F. Dulhunty. Calsequestrin and the calcium release channel of skeletal and cardiac muscle. Prog Biophys Mol Biol.Prog. 2004 May;85(1):33-69.

8. Gabriele Assenza, Camillo Autore, Bruno Marino. Hypertrophic cardiomyopathy in a patient with Down's syndrome. Journal of Cardiovascular Medicine. 8(6):463–464.

9. Tong F., Zhang M., Guo X., Shi H., Li L., Guan W., Wang H. Yang s. Expression patterns of SH3BGR family members in zebrafish development. Dev Genes Evol. doi: 10.1007/s00427-016-0552-5.

10. Egeo A, Mazzocco M, Arrigo P, Vidal-Taboada JM, Oliva R, et al. Identification and characterization of a new human gene encoding a small protein with high homology to the proline-rich region of the SH3BGR gene. Biochem Biophys Res Commun. 1998;247:302-306.

11. Mazzocco M, Maffei M, Egeo A, Vergano A, Arrigo P, et al. The identification of a novel human homologue of the SH3 binding glutamic acid-rich (SH3BGR) gene establishes a new family of highly conserved small proteins related to Thioredoxin Superfamily. Gene. 2002;291:233-239.

12. Mazzocco M, Arrigo P, Egeo A, Maffei M, Vergano A, et al. A novel human homologue of the SH3BGR gene encodes a small protein similar to Glutaredoxin 1 of Escherichia coli. Biochem Biophys Res Commun. 2001;285:540-545.

13. Majid SM, Liss AS, You M, Bose HR. The suppression of SH3BGRL is important for v-Rel-mediated transformation. Oncogene. 2006;25:756-768.

14. H Wang, B Liu, AQO Al-Aidaroos, H Shi, L Li, K Guo, J Li, BCP Tan, JM Loo , JP Tang, M Thura and Q Zeng. Dual-faced SH3BGRL: oncogenic in mice, tumor suppressive in humans. Oncogene (2016). 0950-9232/16.

15. Muñiz Lino MA, Palacios-Rodríguez Y, Rodríguez-Cuevas S, Bautista-Piña V, Marchat LA, et al. Comparative proteomic profiling of triple-negative breast cancer reveals that up-regulation of RhoGDI-2 is associated to the inhibition of caspase 3 and caspase 9. J Proteomics. 2014;111:198-211.

16. Werner CJ, Heyny-von Haussen R, Mall G, Wolf S. Proteome analysis of human substantia nigra in Parkinson's disease. Proteome Sci. 2008;6:8.

17. Evangelia Vakalopoulou, Jerome Schaack, Thomas Shenk. A 32-Kilodalton Protein Binds to AU-Rich Domains in the 3' Untranslated Regions of Rapidly Degraded mRNAs. MOLECULAR AND CELLULAR BIOLOGY. 0270-7306/91/063355-7306/91/063355-10$02.00/0.

18. Yan Cai, Seong Soo, Sang Yun Kim. Mutations in presenilin 2 and its implications in Alzheimer's disease and other dementiaassociated disorders. Clinical Interventions in Aging.

19. Lei Yina, Wenjia Lib, Aiming Xuc, Heng Shia, Keyi Wanga, Huan Yangd, Ronghao Wange, Bo Penga. SH3BGRL2 inhibits growth and metastasis in clear cell renal cell carcinoma via activating hippo/TEAD1-Twist1 pathway. EBioMedicine 52 (2020) 102641

20. Nardini M, Mazzocco M, Massaro A, Maffei M, Vergano A, et al. Crystal structure of the glutaredoxin-like protein SH3BGRL3 at 1.6 Angstrom resolution. Biochem Biophys Res Commun. 2004;318:470-476.

21. Xu C, Zheng P, Shen S, Xu Y, Wei L, et al. NMR structure and regulated expression in APL cell of human SH3BGRL3. FEBS Lett. 2005;579:2788-2794.

22. Chistropher Horst Lilling, Carsten Berndt, Arne Holmgren. Glutaredoxin systems. Biochimica et Biophysica Acta 1780 (2008) 1304-1317.

23. Wang W, Wang S, Zhang M. Identification of urine biomarkers associated with lung adenocarcinoma. Oncotarget (2017) Jun 13;8(24):38517-38529

24. Wu CC, Lin JD, Chen JT, Chang CM, Weng HF, Hsueh C, Chien HP, Yu JS. Integrated analysis of fine-needle-aspiration cystic fluid proteome, cancer cell secretome, and public transcriptome datasets for papillary thyroid cancer biomarker discovery. Oncotarget (2018) Jan 4;9(15):12079-12100.

25. Sanchez C., Mazzucchelli G., Lambert C., Comblain F., DePauw E., Henrotin Y. omparison of secretome from osteoblasts derived from sclerotic versus non-sclerotic subchondral bone in OA: A pilot study. PloS One 2018; 13(3): e0194591.

26. Chiang CY, Pan CC, Chang HY, Lai MD, Tzai TS, et al. SH3BGRL3 Protein as a Potential Prognostic Biomarker for Urothelial Carcinoma: A Novel Binding Partner of Epidermal Growth Factor Receptor. Clin Cancer Res. 2015;21:5601-5611.

27. Kristine Raaby Jakobsen, Emilie Sørensen, Karin Kathrine Brøndum, Tina Fuglsang Daugaard, Rune Thomsen and Anders Lade Nielsen. Direct RNA sequencing mediated identification of mRNA localized in protrusions of human MDA-MB-231 metastatic breast cancer cells. Journal of Molecular Signaling2013.

28. De La Cruz EM, Ostap EM. Relating biochemistry and function in the myosin superfamily. Curr Opin Cell Biol. 2004;16:61-67.

29. Krendel M, Mooseker MS. Myosins: tails (and heads) of functional diversity. Physiology (Bethesda). 2005;20:239-251.

30. Bähler M, Rhoads A. Calmodulin signaling via the IQ motif. FEBS Lett. 2002;513:107-113.

31. Chin D, Means AR. Calmodulin: a prototypical calcium sensor. Trends Cell Biol. 2000;10:322-328.

32. Woolner S, Bement WM. Unconventional myosins acting unconventionally. Trends Cell Biol. 2009;19:245-252.

33. McConnell RE, Tyska MJ. Leveraging the membrane - cytoskeleton interface with myosin-1. Trends Cell Biol. 2010;20:418-426.

34. Lu Q, Li J, Ye F, Zhang M. Structure of myosin-1c tail bound to calmodulin provides insights into calcium-mediated conformational coupling. Nat Struct Mol Biol. 2015;22:81-88.

35. Bähler M, Rhoads A. Calmodulin signaling via the IQ motif. FEBS Lett. 2002;513:107-113.

36. Tang N, Lin T, Yang J, Foskett K. CIB1 and CaBP1 bind to the myo1c regulatory domain. J Muscle Res Cell Motil. 2007 ; 28(6): 285–291. doi:10.1007/s10974-007-9124-7.

37.Lu Q, Li J, Ye F, Zhang M. Structure of myosin-1c tail bound to calmodulin provides insights into calcium-mediated conformational coupling. Nat Struct Mol Biol. 2015;22:81-88.

38. Bose A, Robida S, Furcinitti PS, Chawla A, Fogarty K, et al. Unconventional myosin Myo1c promotes membrane fusion in a regulated exocytic pathway. Mol Cell Biol. 2004;24:5447-5458.

39. Phillips KR, Tong S, Goodyear R, Richardson GP, Cyr JL. Stereociliary myosin-1c receptors are sensitive to calcium chelation and absent from cadherin 23 mutant mice. J Neurosci. 2006;26:10777-10788.

40. Arif E, Wagner MC, Johnstone DB, Wong HN, George B, et al. Motor protein Myo1c is a podocyte protein that facilitates the transport of slit diaphragm protein Neph1 to the podocyte membrane. Mol Cell Biol. 2011;31:2134-2150.

41. Stauffer EA, Scarborough JD, Hirono M, Miller ED, Shah K, et al. Fast adaptation in vestibular hair cells requires myosin-1c activity. Neuron. 2005;47:541-553.

42. Gillespie PG, Cyr JL. Myosin-1c, the hair cell's adaptation motor. Annu Rev Physiol. 2004;66:521-545.

43. Hirono M, Denis CS, Richardson GP, Gillespie PG. Hair cells require phosphatidylinositol 4,5-bisphosphate for mechanical transduction and adaptation. Neuron. 2004;44:309-320.

44. Boguslavsky S, Chiu T, Foley KP, Osorio-Fuentealba C, Antonescu CN, et al. Myo1c binding to submembrane actin mediates insulin-induced tethering of GLUT4 vesicles. Mol Biol Cell. 2012;23:4065-4078.

45. Chen XW, Leto D, Chiang SH, Wang Q, Saltiel AR. Activation of RalA is required for insulin-stimulated Glut4 trafficking to the plasma membrane via the exocyst and the motor protein Myo1c. Dev Cell. 2007;13:391-404.

46. Yip MF, Ramm G, Larance M, Hoehn KL, Wagner MC, et al. CaMKII-mediated phosphorylation of the myosin motor Myo1c is required for insulin-stimulated GLUT4 translocation in adipocytes. Cell Metab. 2008;8:384-398.

47. Capmany A., Yoshimura A., Kerdous R., Caorsi V., Aurianne Lescure, Del Nery E., Coudrier E., Goud B, Schauer K. MYO1C stabilizes actin and facilitates the arrival of transport carriers at the Golgi complex. Journal of Cell Science. 2019 132: jcs225029 doi: 10.1242/jcs.225029.

48. Kittelberger N., Breunig M., Martin R., Knolker H.J., Miklavc P. The role of myosin 1c and myosin 1b in surfactant exocytosis J. Cell S129(8): 1685–1696.

49. Brandstaetter H, Kendrick-Jones J, Buss F. Molecular roles of Myo1c function in lipid raft exocytosis. Commun Integr Biol. 2012;5:508-510.

50. Brandstaetter H, Kendrick-Jones J, Buss F. Myo1c regulates lipid raft recycling to control cell spreading, migration and Salmonella invasion. J Cell Sci. 2012;125:1991-2003.

51. Maravillas-Montero J. L., Gillespie P.G., Patiño-López G., Santos-Argumedo S.S., Santos-Argumedo L. Myosin 1c Participates in B Cell Cytoskeleton Rearrangements, Is Recruited to the Immunologic Synapse, and Contributes to Antigen Presentation. J Immunol. 187 (6) 3053-3063.

52. Wang FS, Liu CW, Diefenbach TJ, Jay DG. Modeling the role of myosin 1c in neuronal growth cone turning. Biophys J. 2003;85:3319-3328.

53. William’s Elong Edimo, Ana Raquel Ramos, Somadri Ghosh, Jean-Marie Vanderwinden, Christophe Erneux. The SHIP2 interactor Myo1c is required for cell

migration in 1321 N1 glioblastoma cells. Biochemical and Biophysical Research Communications 476 (2016) 508e514.

54. Yi Fan, Sandeepa M. Eswarappa, Masahiro Hitomi, Paul L. Fox. Myo1c facilitates G-actin transport to the leading edge of migrating endothelial cells. jcb.201111088.

55. Schulze WX, Deng L., Mann M. Phosphotyrosine interactome of the ErbB-receptor kinase family. Mol Syst Biol. 2005;1:2005.0008. Epub 2005 May 25.

56. Takamitsu Sasaki, Kuniyasu Hiroki and Yuichi Yamashita. The Role of Epidermal Growth Factor Receptor in Cancer Metastasis and Microenvironment. Hindawi Publishing Corporation BioMed Research International Volume 2013, Article ID 546318.10.1155/2013/546318.

57. Nicola Normanno Antonella De Luca, Caterina Bianco, Luigi Strizzi, Mario Mancino, Monica R. Maiello, Adele Carotenuto, Gianfranco De Feo, Francesco Caponigro, David S. Salomon. Epidermal growth factor receptor (EGFR) signaling in cancer. Elsevier. Gene 366 (2006) B.V.doi:10.1016/j.gene.2005.10.018.

58. Pesenti Elisa. Functional characterization of proteins belonging to the SH3BGR family. Doctoral Thesis (University of Genoa), 2017.

59. P. Silacci, L. Mazzolai, C. Gauci, N. Stergiopulos, H. L.Yin and D. Hayoz. Gelsolin superfamily proteins: key regulators of cellular functions. CMLS, Cell. Mol. Life Sci. 61 (2004) 2614–2623.

60. Di Pisa Filippo. Myo1c IQ domains play a role in the interaction with SH3BGRL3 protein. Thesis of Bachelor Degree (University of Genoa), 2014.

61. Di Pisa Filippo. SH3BGRL3 role in the invasive process of tumor cell lines. Thesis of Master Degree (University of Genoa), 2016.

62. Yanling Chen. Transwell Cell Migration Assay Using Human Breast Epithelial Cancer Cell. bio-protocol. 2011

63. Matthew Cardinal, David E. Eisenbud, Tania Phillips, Keith Harding. Early healing rates and wound area measurements are reliable predictors of later complete wound closure. DOI:10.1111/j.1524-475X.2007.00328.

64. Bela Ozsvari, John R. Nuttal, Federica Sotgia, Michael P. Lisanti. Azithromycin and Roxithromycin define a new family of “senolytic” drugs that target senescent human fibroblasts. Aging, 2018.

65. Marco Fiorillo, Rosa Sanchez-Alvarez, Federica Sotgia and Michael P. Lisanti. The ER-alpha mutation Y537S confers Tamoxifen-resistance via enhanced mitochondrial metabolism, glycolysis and Rho-GDI/PTEN signaling: Implicating TIGAR in somatic resistance to endocrine therapy. AGING 2018, Vol. 10, No. 12.

66. Shaw FL, Harrison H, Spence K, Ablett MP, Simões BM, Farnie G, Clarke RB. A detailed mammosphere assay protocol for the quantification of breast stem cell activity. J Mammary Gland Biol Neoplasia. 2012; 17:111–17.

67. Ernestina Marianna De Francesco, Gloria Bonuccelli, Marcello Maggiolini, Federica Sotgia and Michael P. Lisanti. Vitamin C and Doxycycline: A synthetic lethal combination therapy targeting metabolic flexibility in cancer stem cells (CSCs). Oncotarget, 2017.

68. Richard M. Neve, Koei Chin, Jane Fridlyand, Jennifer Yeh, Frederick L. Baehner, Tea Fevr, Laura Clark, Nora Bayani, Jean-Philippe Coppe1 Frances Tong, Terry Speed, Paul T. Spellman, Sandy DeVries, Anna Lapuk, Nick J. Wang, Wen-Lin Kuo, Jackie L. Stilwell, Daniel Pinkel, Donna G. Albertson, Frederic M. Waldma, Frank McCormick, Robert B. Dickson, Michael D. Johnson, Marc Lippman, Stephen Ethier, Adi Gazdar, and Joe W. Gray. A collection of breast cancer cell lines for the study of functionally distinct cancer subtypes. Cancer Cell. 2006 December; 10(6): 515–527. doi:10.1016/j.ccr.2006.10.008

69. Alexander Mogilner and George Oster. Cell Motility Driven by Actin Polymerization.Biophys J. 71(6): 3030–3045. doi:10.1016/S0006-345(96)79496-1

70. Jing Zhao, Juan Zhang, Meifang Yu, Yan Xie, Youguo Huang, Dennis W. Wolff, Peter W. Abel, and Yaping Tu. Mitochondrial dynamics regulates migration and invasion of breast cancer cells. Oncogene. 2013. 32(40): 4814–4824.

71. Andrew Paul Trotta, and Jerry Edward Chipuk. Mitochondrial Dynamics As Regulators Of Cancer Biology. Cell Mol Life Sci. 2017.10.1007/s00018-016-2451-3.

72. Matthew R. Zanotellia, Zachary E. Goldblatta, Joseph P. Millera, Francois Bordeleaub, Jiahe Lia, Jacob A. VanderBurgha, Marsha C. Lampia, Michael R. Kinga and Cynthia A. Reinhart-King. Regulation of ATP utilization during metastatic cell migration by collagen architecture. MBoC (http://www .molbiolcell.org/cgi/doi/10.1091/mbc.E17-01-0041).

73. Vi Ley Chin, Chooi Ling Lim. Epithelial-mesenchymal plasticity—engaging stemness in an interplay of phenotype. Stem Cell Investigation. 10.21037/sci.2019.08.08

74. Panagiotis B., Spyros S. S., Zoi P., Nikos A., Konstantina K.,b, Alexios J. A., Aristidis M. , Achilleas D. T. and Nikos K. K. Estrogen receptor alpha mediates epithelial to

mesenchymal transition, expression of specific matrix effectors and functional properties of breast cancer cells. Elsevier B.V. 10.1016/j.matbio.2015.02.008

75. Estrogen receptor-alpha silenced MCF-7 breast cancer cells, Geo Profile.

76. Kelly Graham, Xijin Ge, Antonio de las Morenas, Anusri Tripathi, and Carol L. Rosenberg. Gene Expression Profiles of Estrogen Receptor–Positive and Estrogen Receptor–Negative Breast Cancers Are Detectable in Histologically Normal Breast Epithelium. Human Cancer Biology. DOI: 10.1158/1078-0432.CCR-10-1369.

77. Pelin Yaşar, Gamze Ayaz, Sırma Damla User, Gizem Güpür, Mesut Muyan. Molecular mechanism of estrogen–estrogen receptor signalling. DOI: 10.1002/rmb2.12006

78. Dionysia Lymperatou, Efstathia Giannopoulou, Angelo K. Koutras, and Haralabos P. Kalofonos. The Exposure of Breast Cancer Cells to Fulvestrant and Tamoxifen Modulates Cell Migration Differently. BioMed Research International. 10.1155/2013/147514.

79. V. Craig Jordan. The role of tamoxifen in the treatment and prevention of breast cancer. Elsevier. 10.1016/0147-0272(92)90002-6

80. Jack Cuzick, Ivana Sestak, Simon Cawthorn, Hisham Hamed, Kaija Holli, Antony Howell, John F. Forbes. Tamoxifen for prevention of breast cancer: extended long-term follow-up of the IBIS-I breast cancer prevention trial. Lancet Oncol. 2015 Jan; 16(1): 67–75.10-1016/S1470-2045(14)71171-4.

81. Peter G Gillespie and Janet L Cyr. Calmodulin binding to recombinant myosin-1c and myosin-1c IQ peptides. BMC Biochemistry 2002, 3:31.

82. Mark A. Eckert and Jing Yang. Targeting invadopodia to block breast cancer metastasis. Oncotarget, 2011.

83. William's Elong Edimo, Ana Raquel Ramos, Somadri Ghosh, Jean-Marie Vanderwinden, Christophe Erneux. The SHIP2 interactor Myo1c is required for cell migration in 1321 N1 glioblastoma cells. Biochemical and Biophysical Research Communications 476 (2016) 508e514.

84. Wenjuan Tian, Shanshan Liu and Burong. Potential Role of Exosomes in Cancer Metastasis. Hindawi BioMed Research International. Article ID 4649705. 10.1155/2019/4649705.

85. Yu-Ling Tai, Ko-Chien Chen, Jer-Tsong Hsieh, Tang-Long Shen. Exosomes in cancer development and clinical applications. Wiley Cancer Science. DOI: 10.1111/cas.13697.

86. Joana Monteiro, Riccardo Fodde, Cancer stemness and metastasis: Therapeutic consequencesand perspectivesa. Elsevier, EUROPEAN JOURNAL OF CANCER 46 (2010) 1198 – 1203.

87. Matthew R. Zanotellia, Zachary E. Goldblatta, Joseph P. Millera, Francois Bordeleaub, Jiahe Lia, Jacob A. VanderBurgha, Marsha C. Lampia, Michael R. Kinga,b, and Cynthia A. Reinhart-King. Regulation of ATP utilization during metastatic cell migration by collagen architecture. MBoC | BRIEF REPORT.

88. I. K, Guttilla, K.N. Phoenix, X. Hong, J. S. Tirnauer, K. P. Claffey and B. A. White. Prolonged mammosphere culture of MCF-7 cells induces an EMT and repression of the estrogen receptor by microRNA. Breast Cancer Research and Treatment. Volume 132, pages75–85(2012).

ACKNOWLEDGEMENT

First of all, I would like to express my gratitude to all the Laboratory of Molecular Immunology and Oncology (MIaO Lab, University of Genoa) members and to my supervisor Fabio Ghiotto for their motivation, advises and guidance.

In particular, a very special gratitude goes to Claudya Tenca and Elenina, their helpful, support and suggestions were very precious to me. They were not just colleagues, they were more. They were friends, and friends are essential. Among this I would like to thank Grazia Bellese, a cigarette with a good company can make easier everything, also work times.

Many thanks to the Biochemistry Lab (University of Genoa), specially to Elena Laugeri for her helpful, supporting and wonderful times together.

I would also like to acknowledge Michael P. Lisanti and Federica Sotgia (University of Salford) for giving me this great possibility to have a wonderful experience, for their valuable advises, patience and knowledge.

Very special gratitude goes to Gloria Bonuccelli and to all the fantastic people of the Translational Medicine Lab: Rumana, Marco, Bela, and John.

To Fanni, for all the food we shared together. Isn't this friendship?

To Ernestina and Alessandra, I wish we could work together again.

In particular, to Sonia, Marta and Camillo for our good times and adventures we shared.

Sincere thank goes to my friends, that are my family. To Annalinda, Camilla and Andrea. With all my love, I thank you. To the little Tommaso, I wish all my best to you.

To Luisa, you got the best laugh I've ever heard.

To Matelda, that every time reminds me to don't stop to believe in love.

Particularly thank goes to Alessia, Francesca and Emanuele for all your suggestions.

I would like to thank my special "aunts" Giulia and Silvia for all your precious advices.

Heartfelt thanks go to Margherita and Francesca, you helped me, *always*. I wish I could do the same for you.

A special thank goes to Raffa, you taught me that happiness can be found in simplicity as a homemade cake shared with all your little women. I wish I could be like you one day.

To Lorella Gasparini, my marvellous secondary school teacher, for all her support.

To my fool friend Silvietta, you are amazing. I enjoyed every time I spent with you.

To Dott.ssa Fabrizia Fiandesio, thank you to brought me to discover the world and myself.

To my parents, and my family. To Eleonora for all her support.

Finally, cause the very essential things need to tell at the end, I would like to say thank with all my heart to Paolo Scartezzini. Thanks to yours advises and immense knowledge. You taught me everything, you believed me, you supported me and you encouraged me. As a grandfather does, you've never doubted about me and this gave me the strength to carry on and go *over*.

Manchester (UK) 14.11.19,

Filippo